# Peierls and Spin-Peierls Instabilities in the $Per_2[M(mnt)_2]$ Series of One-Dimensional Organic Conductors; Experimental Realization of a 1D Kondo Lattice for M = Pd, Ni and Pt

**Jean-Paul Pouget [1], Pascale Foury-Leylekian [1], and Manuel Almeida [2]**

[1] Laboratoire de Physique des Solides, Université Paris-sud, CNRS UMR 8502, F91405 Orsay, France

[2] C2TN - Centro de Ciências e Tecnologias Nucleares, Instituto Superior Técnico, Universidade de Lisboa, P-2695-066 Bobadela LRS, Portugal

**Abstract**

We summarize structural instabilities exhibited by the one dimensional (1D) $(arene)_2X$ family of organic conductors in relation with their electronic and magnetic properties. With a charge transfer of one electron to each anion X these salts exhibit a quarter-filled (hole) conduction band located on the donor stacks. Compounds built with donors such as fluorenthene and perylene derivatives and anions X such $PF_6$ or $AsF_6$ exhibit a high temperature ($T_P$~170K) conventional Peierls transition which is announced by a sizeable regime of 1D $2k_F$ charge density wave fluctuations ($k_F$ is the Fermi wave vector of the 1D electron gas located on Per stacks). Surprisingly, and probably because of the presence of a multi-sheet warped Fermi surface, the Peierls transition is considerably reduced in the perylene series $\alpha$-$(Per)_2[M(mnt)_2]$ where X is the dithiolate molecule with M=Au, Cu, Co and Fe. A special attention is devoted in this paper to physical properties of $\alpha$-$(Per)_2[M(mnt)_2]$ salts which with M=Pt, Pd and Ni incorporate segregated S=1/2 1D antiferromagnetic (AF) dithiolate stacks with 1D metallic Per stacks. We analyse conjointly the structural and magnetic properties of these salts in relation with the 1D spin-Peierls (SP) instability located on the dithiolate stacks. We show that the SP instability of the Pd and Ni derivatives occurs in the classical (adiabatic limit) while the SP instability of the Pt derivative occurs in the quantum (anti-adiabatic limit). Furthermore we show that in the Pd and Ni derivatives frustrated 1st neighbour direct and 2nd neighbour indirect (through a fine tuning with the mediated $2k_F$ RKKY coupling interaction on Per stacks) AF interactions add their contribution to the SP instability to open a singlet-triplet gap. Our analysis of the data show unambiguously that magnetic $\alpha$-$(Per)_2[M(mnt)_2]$ salts are a typical realization of the physics predicted for two chain 1D Kondo lattices.

**Keywords:** organic conductors; one dimensional metal; Kondo lattice; Peierls and spin-Peierls transitions; frustrated anti-ferromagnetic systems

---

## I- Introduction

Since the discovery of a so-called Peierls transition in the Krogmann salt $K_2Pt(CN)_4Br_{0.3}$-$3H_2O$ (KCP) [1] in 1973, more than 40 years ago, a lot of investigations have shown that most of one dimensional (1D) conductors are subject to a coupled electronic-structural instability transition at the $2k_F$ critical wave vector ($k_F$ being the Fermi wave vector of the 1D electron gas). Due to the electron-phonon coupling the Peierls transition consists in a $2k_F$

modulated wave of bond distances, forming a so-called bond ordered wave (BOW), accompanied by a $2k_F$ modulation of the electronic density, forming a so-called charge density wave (CDW); these two waves being in quadrature (see [2]). This $2k_F$ modulation adjusted to the 1D band filling is generally in incommensurate relation with the chain reciprocal wave vector, b* below ($2k_F$ amounts to half the number of conduction electrons, ρ, per site in b* reciprocal unit; the factor 2 is due to the spin degree of freedom). At the Peierls transition, $T_P$, the long range $2k_F$ modulation opens a gap at the Fermi level in the 1D band structure, which leads to a 1D metal to insulator phase transition. However because of the 1D nature of the electronic instability, the Peierls instability is announced by a large regime of 1D $2k_F$ CDW/BOW fluctuations which extends up to 2-4 times $T_P$ (the temperature of onset of CDW/BOW fluctuations corresponds to about the mean-field Peierls temperature, $T_P^{MF}$). Between $T_P^{MF}$ and $T_P$ these local fluctuations in direct space open a partial gap (i.e. a pseudo-gap) in the electronic structure. More details can be found in a recent review [3].

These $2k_F$ CDW instabilities are well illustrated by quasi-1D inorganic compounds such as the Krogmann salts, the blue bronzes, $K_{0.3}MoO_3$, and the transition metal tri-chalcogenides, $NbSe_3$ and $TaS_3$, built with chain of transition elements based inorganic polyhedron ($PtCN_4$ square, $MoO_6$ octahedron and $NbSe_6$/$TaS_6$ anti-prism, respectively) between which there is a strong overlap of d wave functions [4]. Organic conductors are built with stacks of planar molecules with a sizeable overlap of $p_\pi$ perpendicular molecular orbitals (MO). In them the metallic character is achieved either by a partial charge transfer ρ from stacks of donor (D) to stacks of acceptor (A), as in TTF-TCNQ, or by a complete charge transfer from anion (X)/cation (Y) to D/A in 2:1 $D_2X$ or $A_2Y$ salts. Only the $D_2X$ salts where, with ρ=1/2 the hole band structure is quarter-filled, will be considered in this paper. An important characteristic of organic metals is that, with stacks built with large planar molecules, the HOMO have a nodal structure which gives intra-stack transfer integral ($t_{//}$) often smaller or comparable to intra-molecular (U) or inter-molecular (V) Coulomb repulsion terms. Thus because of the relative importance of electron repulsion, the organic conductors have a strong tendency to develop another type of CDW instability at the critical $4k_F$ wave vector consisting in a Wigner like charge localization [2] (charge localization is generally accompanied by a spin-charge decoupling. Thus a given site can be at most occupied by an electron whatever its spin. The critical wave vector in this process, being associated to ρ, is $4k_F$ in 1D). In 2:1 organic salts, intensively studied these last year [5], a spin-charge decoupling accompanies the charge localization phenomenon. When such a decoupling is achieved, the localized S=1/2 degrees of freedom remain available to order in magnetic such as anti-ferromagnetism (AF) or non-magnetic singlet paired ground states. The singlet pairing is generally stabilized by a dimerization of the chain of localized spins. The transition which results thus opens a singlet-triplet gap in the AF magnetic excitation spectrum. Being analogue to the metal-insulator Peierls transition, which opens a gap in a metallic excitation spectrum, the singlet pairing transition of spins 1/2 is called for this reason a spin-Peierls (SP) transition whose principal characteristics are now well documented by the recent literature (see for example ref. [3, 5]).

The perylene (Per) molecule, shown in figure 1a, has played an important role in the development of the field of 1D organic conductors since the first molecular crystal exhibiting a metallic conductivity was found in 1954 when Per was exposed to Br [6]. Then many family of organic salts based on the Per donor and its derivatives were found to exhibit metallic properties [7]. Among them 2:1 $D_2X$ salts were found to exhibits quasi-1D metals exhibiting a $2k_F$ BOW/CDW instability diverging into a Peierls metal-insulator transition (see section

Preprints (www.preprints.org) | NOT PEER-REVIEWED | Posted: 26 January 2017 doi:10.20944/preprints201701.0118.v1

Peer-reviewed version available at Magnetochemistry 2017, 3, 13; doi:10.3390/magnetochemistry3010013



II). A very original physics is observed in Per-dithiolate salts α-$(Per)_2[M(mnt)_2]$ which for some specific dithiolate acceptors mix 1D conducting and magnetic properties [7, 8].The structure of α-$(Per)_2[M(mnt)_2]$ exhibits along the b direction (perpendicular to the plane of figure 2) regular stacks of tilted and partially oxidized Per molecules which coexist with metal-bisdithiolene complex $[M(mnt)_2]^-$ stacks. $[M(mnt)_2]^-$, shown in figure 1b, is a close shell molecule for M=Au and Cu while for M = Ni, Pd and Pt each $[M(mnt)_2]^-$ bears an unpaired spin 1/2. Due to the charge transfer of one electron per dithiolate leaving ρ=1/2 hole per Per, α-$(Per)_2[M(mnt)_2]$ forms a family of high conducting and anisotropic conductors ($\sigma_b$ ~700S/cm and $\sigma_b/\sigma_\perp \sim 10^3$ at RT) [9] with a quarter-filled hole (or a three quarter filled electron) conduction band – see figure 3a. With M=Au and Cu close shell dithiolate molecules and with M=Fe and Co dithiolate molecules forming stacks of dimers, only the Per stack is electro-active. The Peierls instability of these salts will be considered in section II and compared to the Peierls instability exhibited by other $D_2X$ salts of arene donors. Dithiolate stacks with M = Ni, Pd and Pt form S=1/2 AF chains which interact with the conducting Per stacks, subject to a Peierls instability similar to the one exhibited by Per stacks in the close shell dithiolate salts. These very interesting systems will be considered separately in section III since a new physics emerges from the coupling between magnetic and metallic stacks.

## II- Peierls instability in $Per_2X$ salts and its Per substituted derivatives

In this section we summarize the Peierls instabilities exhibited by various $D_2X$ arene cation radical salts whose main characteristics are given in table I. This table shows that depending of the salt the donor stacking can be either uniform or two-fold modulated. In the second case two-fold bond or site modulation of the donor stack is generally the consequence of differentiated interactions with either intrinsically dimerized anionic stacks or chemically alternated anion-solvant columns. These differentiated interactions should change donor environment with respect to the one in regular stacks. These differential interactions will either modulate intra-stack bond distances and/or modulate the molecular site potential with the consequence to modulate electronic parameters such as either the intra-stack transfer integral or the one-electron site energy (see figure 3b). In all these cases there is a band folding in b*/4 or b'*/2 and the opening of a band gap of $2E_G$ as shown in figure 3b, which gives also the expression of $E_G$. Furthermore if there is a lateral disorder between columns of anions the modulation of donor stack located between these columns will be also disordered.

1D CDW are very sensitive to disorder. Disorder either limits the life time of electron-hole pairs of wave vector $2k_F$, which are the building blocks of the CDW, or pins the phase of the BOW/CDW modulation. Electron backscattering on impurities reverses the wave vector of one constituent of the electron-hole pair (let say from $+k_F$ to $-k_F$), which process destroies the pairing. In consequence such a scattering process gives a finite lifetime at the electron-hole pairing. This lifetime effect depresses the Peierls transition, as observed in the solid solution $Per_2[Au_xPt_{1-x}(mnt)_2]$ [11]. Local pinning of the phase of the CDW on a random distribution of lattice defects limits the longitudinal and transverse spatial coherence of the 3D CDW order (for more details see [3]).

### a- Uniform stack

For ρ=1/2 hole per arene the 1D donor band structure is quarter-filled in holes (¾ filled in electrons) - figure 3a. For an uniform stack of periodicity b, the critical Peierls wave vector is $2k_F^D$= b*/4 for the hole filling ($2k_F^D$= 3b*/4 for the electron filling). In the mean field

Preprints (www.preprints.org) | NOT PEER-REVIEWED | Posted: 26 January 2017 doi:10.20944/preprints201701.0118.v1

Peer-reviewed version available at Magnetochemistry 2017, 3, 13; doi:10.3390/magnetochemistry3010013



approximation (which neglects the 1D pre-transitional $2k_F^D$ fluctuations) the Peierls transition occurs at:

$$T_P^{MF} \approx C\, E_F e^{-1/\lambda_{2k_F}} \quad (1)$$

In (1) $E_F$ is the hole Fermi energy and, since $2k_F$ phonons pair a $-k_F$ hole to a $+k_F$ electron, $\lambda_{2k_F}$ is the reduced $2k_F$ electron-phonon coupling [3]. C is a constant, of few units, which depends on the shape of the band dispersion in the vicinity of $E_F$ (for a free electron dispersion C≈2.25). The Peierls transition opens a gap 2Δ at $\pm k_F$ in the 1D band structure. At 0K, the gap $2\Delta_0$ is related to $T_P^{MF}$ by the BCS-type correspondence law:

$$2\Delta_0 = 3.56 T_P^{MF} \quad (2)$$

Table I reports $T_P^{MF}$ deduced, via expression (2), from the activation energy $\Delta_0$ of the conductivity measured below $T_P$.

Note that with $2k_F^D = b^*/4$, the Peierls superstructure stabilizes a 4b periodicity in stack direction. Since $4 \times 2k_F^D = b^*$, the $2k_F$ BOW/CDW modulation wave length is in fourth-fold commensurate relation with the chain periodicity b, so that the phase of the CDW modulation should be pinned on lattice sites by the fourth-order lattice potential.

**b- Two-fold modulated stack**

Table I shows that in many salts the donor stack periodicity is doubled. In that case with a stack periodicity of b'=2b, the critical Peierls wave vector should be $2k_F^D = b'^*/2$ (see the folded band structure shown in figure 3b). Note also that the new reciprocal wave vector b'* of the two-fold modulated structure amounts to $4k_F^D$ which is the critical wave vector associated to a charge localization phenomena (see above). In that case the band folding opens a band gap $2E_G$ in $\pm b'^*/2$ due either to a dimerization of the stacks or to the presence of non-equivalent lattice sites. Generally the bond dimerization due to molecular shifts ±u/2 (leading to a difference of transfer integral $\delta t = g_B u$) or the charge unbalance on each site ±δρ (related to a difference of HOMO potential energy $\delta V = g_S \delta\rho$) are small quantities, so that with $E_G = 2\delta t$ or $E_G = \delta V$ one has $E_G \ll t$. In these expressions $g_i$ is the bond (B) or site (S) electron-phonon coupling and t is the transfer integral of the uniform stack. Note that in these cases the underlying dimerization or charge modulation effects, can be viewed as achieved by the establishment of a static $4k_F$ BOW or $4k_F$ CDW of amplitude u/2 or δρ respectively on the Per stack. For a weak modulation and for a weakly interacting electron gas, these effects does not change appreciably the physics of the Peierls instability with respect to the one of a quarter-filled band. In particular the $2k_F$ BOW/CDW modulation should remain mainly pinned on lattice sites by a fourth-order lattice potential as for a uniform stack (the two-fold order lattice potential proportional to u or δρ being much smaller). This is not true for a strong modulation in presence of sizeable electron repulsions (see for example [5]).

In the case of a strong dimerization shown in figure 3c, where $t_{intra} \gg t_{inter}$, the bonding and anti-bonding states of the dimer are well decoupled. One hole tends to be localized on the anti-bonding state of each dimer, and the anti-bonding band can be considered as half-filled. In this picture each dimer can be considered as a rigid unit and the $2k_F$ BOW/CDW modulation of wave length 2b' will basically modulate the inter-dimers distances. There is thus strong pinning of the CDW on dimer sites by a two-fold lattice potential.

Preprints (www.preprints.org) | NOT PEER-REVIEWED | Posted: 26 January 2017 doi:10.20944/preprints201701.0118.v1

Peer-reviewed version available at Magnetochemistry 2017, 3, 13; doi:10.3390/magnetochemistry3010013



In the case of a two-fold modulated stacks there is an additional process entering in the $2k_F$ electron-phonon coupling mechanism. Since one has $4k_F^D = b'^*$, umklapp scattering processes should contribute to the $2k_F$ electron-phonon coupling mechanism. The associated reduced electron-phonon coupling constant, $\lambda_{um}$, which is proportional to the amplitude of the $4k_F$ BOW or of the $4k_F$ CDW, adds to $\lambda_{2k_F}$ in expression (1). One simply has in the mean-field approximation:

$$T_P^{MF} \approx C\, E_F e^{-1/(\lambda_{2k_F}+\lambda_{um})} \quad (3)$$

In the limit of a strongly dimerized stack the contribution of umklapp processes could be of the same magnitude as the normal $2k_F$ electron-phonon coupling process. In that case with $2\lambda_{2k_F} \approx \lambda_{2k_F} + \lambda_{um}$ one obtains an enhanced mean-field Peierls transition temperature given by:

$$T_P^{MF} \approx C E_F e^{-1/2\lambda_{2k_F}} \quad (4)$$

**c- Estimation of the electron-phonon coupling**

In a 3D solid made of a collection of weakly coupled chains, the 3D Peierls transition temperature, $T_P$, is generally depressed by a sizeable fraction of $T_P^{MF}$ (see table I). The main cause of this depression arises from the presence of 1D structural fluctuations which develop between $T_P$ and about $T_P^{MF}$ [3]. In that temperature range local lattice fluctuations form a pseudo-gap in the electronic density of states, which announces the formation of a true Peierls gap below $T_P$. As the pseudo-gap reduces the effective number of carriers in the vicinity of the Fermi level it is observed a decrease of conductivity below a certain temperature $T_\rho$ close to $T_P^{MF}$ ( see table I) and well above $T_P$. Note that for a purely 1D system the CDW and BOW thermal fluctuations suppress the Peierls transition at finite temperature. The non-zero $T_P$ values reported in Table I correspond to a 3D phase transition due to various kinds of inter-chain coupling mechanisms (for more detail see [3]).

Then using expression (1) or (4) for uniform or strongly two fold modulated stacks it is possible to estimate λ from the knowledge of $T_P^{MF}$ and $E_F$. In α-$(Per)_2[M(mnt)_2]$ the linear thermal dependence of the hole-like thermo-power leads to a bandwidth of $4t_{//}$=0.6eV [7, 8] which gives for a quarter filled 1D hole band $E_F = \sqrt{2}t_{//}$≈0.2eV. Using $T_P^{MF}$≈ $T_\rho$ from table I and taking a free hole dispersion in the vicinity of $E_F$, as assessed by the band structure calculation of ref. [10], one gets using expression (1):

- $\lambda_{2k_F}$~0.2 for the M=Au salt,
- $\lambda_{2k_F}$~0.25 for the M=Cu salt.

Assuming a sizable Per stack dimerization due to the chemical bonding of $M(mnt)_2$ into dimers [12], one gets using expression (4):

-$\lambda_{2k_F}$~0.2 for the M=Fe and Co salts,

These values are comparable to $\lambda_{2k_F}$ found for KCP (0.2) and for the blue bronze $K_{0.3}MoO_3$ (0.25).

If one assumes the same band width in $(FA)_2 PF_6$ as in α-$(Per)_2[M(mnt)_2]$ one gets, assuming that the stack dimerization has weak effects (see below), that $\lambda_{2k_F}$ =0.6. A similar quite strong electron-coupling value of $\lambda_{2k_F}$=0.6 is obtained in the Peierls ground state of polyacetylene, $(CH)_x$.

**d- Peierls instability in (arene)$_2$ PF$_6$ and AsF$_6$ salts**

Table I shows that D$_2$X salts where D is fluoranthene (FA) or perylene substituted derivatives with 4 methyl groups (TMP) or two cyclopentanes (CPP) (see figure 1a) exhibit, in presence of monovalent anions such as X= PF$_6$ and AsF$_6$, an important regime of 1D 2k$_F$ fluctuations pre-transitional to a Peierls transition. Such 1D 2k$_F$ BOW fluctuations, associated to a sizable electron-phonon coupling with the p$_\pi$ electrons, have been clearly detected in the FA, CPP and TMP salts by X-ray diffuse scattering measurements [13, 14, 15, 16]. Figure 4 shows, for example for (CPP)$_2$AsF$_6$+CH$_2$Cl$_2$, that the susceptibility associated to 1D BOW instability follows a Curie-Weiss dependence (corresponding to a regime of Gaussian fluctuations of the amplitude of the order parameter) which diverges at T$_P$=170K into a 2$^{nd}$ order Peierls transition [15]. Similar results are found in (FA)$_2$PF$_6$ [13]. BOW/CDW fluctuations strongly affect the electron density of states at the Fermi level by forming a pseudo-gap, precursor to the Peierls gap. This progressively reduces the effective number of carriers available for the charge transport so that the electrical conductivity decreases in the temperature range of existence of 1D fluctuations below T$_\rho$ (~T$_P^{MF}$). All these features are those of a conventional Peierls instability.

In most of the salts, the BOW/CDW fluctuations couple 3D in a Peierls transition which stabilizes at T$_P$ a 3D long range order (LRO) of BOW/CDW modulations. This 3D Peierls transition manifests by the appearance below T$_P$ of 2k$_F$ superstructure reflections whose intensity is proportional to the square of the amplitude of the BOW/CDW modulation (see figure 4 in the case of (CPP)$_2$AsF$_6$+CH$_2$Cl$_2$ [15]).

In the Peierls ground state it has been observed in dimerized (FA)$_2$PF$_6$ that the BOW/CDW modulation could collective slide under the action of an external electric field exceeding a threshold field value of E$_T$ ~0.2V/cm [17, 18] which comparable to the one (E$_T$~0.5V/cm) observed in α-(Per)$_2$Au(mnt)$_2$ which exhibits a regular Per stack [19]. As the threshold field depends on the pinning energy of the CDW on impurity and on the order of commensurability of the lattice potential, the finding of similar E$_T$ values for (FA)$_2$PF$_6$ and α-(Per)$_2$Au(mnt)$_2$ means that the pinning is mainly achieved by a fourth-order lattice potential in (FA)$_2$PF$_6$. Thus the 2k$_F$ CDW critical wave vector of (FA)$_2$PF$_6$ is basically that of a quarter filled band.

Table I shows that TMP and CPP salts incorporate one solvent molecule (CH$_2$Cl$_2$), S per anion X. This leads to the formation of mixed X-S columns in stack direction with a short range lateral order between X-S columns [16]. In CPP salts, anion disorder does not prevent the occurrence of a high temperature Peierls transition T$_P$ =158-170K (see table I and figure 4). (TMP)$_2$AsF$_6$+CH$_2$Cl$_2$ exhibits also a sizeable regime of 2k$_F$ fluctuations below ~200K, but at the difference of (CPP)$_2$AsF$_6$+CH$_2$Cl$_2$ it exhibits only a short range BOW lateral order at 20K [15]. The absence of a long range 3D BOW order could be due to CDW pinning on X-S disorder. In addition, and by analogy with the finding in [(TMTSF)$_{1-x}$ (TMTTF)$_x$]$_2$ReO$_4$ solid solution [20], the growth of a 2k$_F$ BOW instability could be inhibited by the establishment of a high temperature 4k$_F$ CDW order on the TMP stack.

**e- Peierls instability in Per stack of α-(Per)$_2$[M(mnt)$_2$]**

α-(Per)$_2$[M(mnt)$_2$] salts with M=Au, Cu, Fe and Co exhibit a quite small Peierls distortion which is assessed by the detection below T$_P$ of extremely weak superlattice reflections at the 2k$_F$=1/4b* reciprocal position in the Cu salt [21] and somewhat stronger reflections at the 2k$_F$=1/2b'* reciprocal position in dimerized Fe and Co salts [22]. No superlattice reflections have been detected in the Au salt (however it is expected from the relative magnitude of the

Peierls gap, superlattice reflections one order of magnitude less intense in the Au salt than in the Cu salt). In addition the expected regime of pre-transitional 1D $2k_F$-BOW fluctuations could not be detected in these salts. The characteristics temperature $T_P$, $T_\rho$ and $T_P^{MF}$ of the Peierls instability located on these salts are reported in table I.

The $2k_F=1/4b^*$ CDW stabilized below $T_P$ in the Au compound collectively slides under the action of an external electric field above $E_T$~0.5V/cm and exhibits the characteristic features of non-linear conductivity phenomena observed in CDW inorganic systems such as the blue bronze and the transition metal tri-chalcogenides [19, 23]. Note however that the observation of a much larger threshold field $E_T$~9V/cm in the Pt salt [23] could be explained by the presence of a two-fold lattice pinning potential brought by the SP dimerization of the $[Pt(mnt)_2]$ stacks (see section III).

As expected for a Peierls system, the critical temperature $T_P$ of the Au compound decreases as $H^2$ for modest magnetic fields [24]. More interestingly, and because of its low value of $T_P$, the CDW ground state is found to be unstable for large magnetic fields $H_c$~33-37T exceeding the so-called Pauli limit $H_P \approx$ 22.5T [25, 26]. Also unexpected features are observed near $H_c$ suggesting the occurrence of field induced CDW states due to orbital effects arising from the existence of a warped Fermi surface (FS) [26, 27].

Because of the presence of a two slightly shifted set of double quasi-1D warped FS [10] combined with the opening of a Peierls gap only slightly larger than inter-stack transfer integrals ($t_\perp$ ~2meV), it is expected in the Au compound, as for system exhibiting a warped FS incompletely nested by the $2k_F$ wave vector, a destabilization of the Peierls instability when pressure enhances the nesting breaking components of the FS. More precisely it is calculated [28] that the Peierls ground state should vanishe when $\Delta_0$ becomes smaller than the typical energy of hole and electron pockets remaining after anincomplete FS nesting process. Indeed it has been observed a vanishing of the CDW ground state of the Au compound above $P_c \approx$5kbar. But more interestingly, it is also found, when the low temperature metallic state is restored under pressure, that $\alpha$-$(Per)_2[Au(mnt)_2]$ becomes a superconductor below $T_S$~0.3K [29].

Finally it is interesting to remark that the 0K Peierls gap, $2\Delta_0 \approx 3.5$ meV, is quite small in the Au salt [7, 8]. More quantitatively $\Delta_0$ is smaller than a typical acoustic phonon frequency ($\Omega_c$ ~5.5-8meV in TTF-TCNQ for $2k_F=3/4b^*$ [30]). So with $2\Delta_0 < \hbar\Omega_c$ the Peierls transition of the Au salt should occur in the non-adiabatic regime [31]. In this regime it is expected that $2k_F$ pre-transitional fluctuations, of dynamics governed by $\Omega_c$, are too rapid to affect the one electron density of states above $T_P$. The situation should be different in the Cu where $2\Delta_0 \approx$ 20 meV [7 8]. With $2\Delta_0 > \hbar\Omega_c$ the Peierls transition of the Cu salt should occur in the adiabatic regime, as for the $(arene)_2 PF_6$ and $AsF_6$ salts considered in part (d) above.

Note that in this framework that the 0K amplitude of the Peierls gap in the Au salt should be reduced by quantum fluctuations from the value obtained by the BCS relation-ship (2). Also in this case the non-adiabaticity of the Peierls mechanism should increase under pressure because of the hardening of the frequency of phonon modes. This should also reduce the Peierls gap. In that case the vanishing of the CDW ground state under pressure in the Au salt should occur at a quantum critical point.

Preprints (www.preprints.org) | NOT PEER-REVIEWED | Posted: 26 January 2017 doi:10.20944/preprints201701.0118.v1

Peer-reviewed version available at Magnetochemistry 2017, 3, 13; doi:10.3390/magnetochemistry3010013



### f- Comparison between Peierls instabilities in (arene)$_2$PF$_6$/AsF$_6$ and in α-(Per)$_2$[M(mnt)$_2$] salts

While donor stack of all these different families includes arene molecules of similar shape, there is a sizeable difference between Peierls instabilities in FA and CPP salts and those in Per salts. There is in particular a difference of more than a factor two in the Peierls transition temperature $T_P$ between these two series of salts -and in the magnitude of the temperature range [$T_\rho$-$T_P$] of 1D CDW fluctuations. As seen in table I, $T_\rho$ occurs well above RT for FA and CPP salts, $T_\rho$ is around 160-180K (~2 times $T_P$) for the M=Co and Fe derivative and $T_\rho$ is very close to $T_P$ for the Cu and Au derivatives. Table II shows that in the M=Ni, Pd and Pt derivatives, $T_P$ and $T_\rho$ are comparable to those of the Au and Cu derivatives quoted in table I.

Two explanations can be invoked. One explanation relies on the difference of nature of the anion: octahedral $PF_6^-$ and $AsF_6^-$ simple anions in FA, CPP and TMP salts versus more polarizable dithiolate $[M(mnt)_2]^-$ anions in the α-Per salts. Another explanation relies on the number of donor conduction bands crossing the Fermi level and on their degree of warping: 1 band for CPP and TMP salts, 2 bands for FA salts and 4 bands for Per salts. In the case of α-(Per)$_2$[M(mnt)$_2$] the total FS includes 4 sheets composed of two slightly shifted sets of warped open FS [10]. With such a band structure the best nesting wave vector of the global FS is poorly define. This could smoothen the logarithmic thermal divergence of the $2k_F$ electron-hole response function [28]. A somewhat similar situation is found in the quarter-filled (TSeT)$_2$Cl organic salt, which with a poorly nested FS composed of 4 warped sheets, also exhibits a modest Peierls transition temperature of 26K [32].

| compound | Donor stacking | $T_P$ (K) | $2k_F^D$ BOW pre-transitional fluctuations | $T_\rho$ (K) | $T_P^{MF}$(K) |
|---|---|---|---|---|---|
| Per$_2$[Cu(mnt)$_2$] | Uniform | 32 | not observed | 40 | 66 |
| Per$_2$[Au(mnt)$_2$] | Uniform | 12 | not observed | 16 | 11.5 |
| Per$_2$[Fe(mnt)$_2$] | Dimerized[a] | 73 | 3D ≤ 80K | 180 | 165 |
| Per$_2$[Co(mnt)$_2$] | Dimerized[a] | 58 | 3D ≤ 65K | 160 | 200 |
| (CPP)$_2$PF$_6$+CH$_2$Cl$_2$ | Uniform?[b] | 158 | 1D above RT | >300 | ? |
| (CPP)$_2$AsF$_6$+CH$_2$Cl$_2$ | Uniform?[b] | 170 | 1D above RT | ? | ? |
| (TMP)$_2$PF$_6$+CH$_2$Cl$_2$ | $4k_F$ site CDW[c] | < 20 | 1D ≤ 210K | >300 | ? |
| (TMP)$_2$AsF$_6$+CH$_2$Cl$_2$ | $4k_F$ site CDW[c] | < 20 | 1D ≤ 200K | ? | ? |
| (FA)$_2$ PF$_6$ | Dimerized | 180 | 1D above RT | >300 | 400-600 |

Table I. Cha racteristics of arene cation radical salts exhibiting a Peierls instability. The table gives the crystal structure of the donor stack. The Peierls transition temperature ($T_P$) and the temperature of minimum of resistivity ($T_\rho$) are taken from conductivity measurements of ref. [7, 8]. The mean field Peierls temperature ($T_P^{MF}$) is calculated from the electrical gap $2\Delta_0$ using expression (2). The dimension and temperature range of $2k_F^D$ BOW pre-transitional fluctuations are also indicated.

[a] Dithiolate sacks composed of paired [Fe(mnt)$_2$] or [Co(mnt)$_2$] units should induce a doubling of the Per stack periodicity. The expected Per two-fold stack deformation due to its dimerized surrounding has not been determined in the Co compound [12a], but has been recently determined to be small in the Fe compound [12b].

[b] The question mark leaves open a possible doubling of the CPP stack periodicity induced by the coupling with the staggered anion - solvent order [16].
[c] A doubling of the TMP stack periodicity is expected from the staggered charge order (i.e. $4k_F$ CDW) on donor stack revealed by $^{13}$C-CPAS-NMR [16]. However local NMR measurements are unable to probe the spatial extend of the charge order periodicity.

## III- Peierls and spin-Peierls instabilities in α-(Per)$_2$M(mnt)$_2$] with M = Ni, Pd and Pt

A special attention must be devoted to Per salts incorporating [M(mnt)$_2$] acceptors with M = Ni, Pd and Pt, because the charge transfer from Per to dithiolate complexes leads to the formation of non-close shell [M(mnt)$_2$]$^-$ anions for M = Ni, Pd and Pt. One thus obtains two kinds of electro-active donor and acceptor stacks. However at variance with TTF-TCNQ where the incommensurate charge transfer gives rise to two types of conducting stacks, each subject to its own CDW instability, the [M(mnt)$_2$]$^-$ stack is not conducting because there is a Mott-Hubbard localization of one electron per [M(mnt)$_2$]. With the charge localization each [M(mnt)$_2$]$^-$ molecule bears an unpaired spin ½. One thus obtains S=1/2 AF dithiolate chains which coexist with metallic Per stacks in the α-type structure (figure 2). As for the M=Au and Cu derivatives, Per stacks of the Pt, Pd and Ni derivatives are subject to a Peierls instability whose main characteristics ($T_P$ and $T_\rho$) are given in table II.

At this stage it is interesting to remark that when there is an incommensurate charge transfer of 0.82 electron from Li to [Pt(mnt)$_2$]$^-$ dithiolate stacks, the 1D conductor Li$_{0.82}$[Pt(mnt)$_2$](H$_2$0)$_2$, resembling to some extend to KCP, undergoes a conventional Peierls transition at $T_P$=215K announced by a sizeable regime of $2k_F$ BOW fluctuations [33]. These data mean that the Peierls instability of dithiolate stacks is achieved by a sizeable electron-phonon coupling. Such critical phonon modes should play a role, via the magneto-elastic spin-phonon coupling, in S=1/2 AF electron localized [M(mnt)$_2$] chains. This coupling is the basic ingredient allowing to transmit the SP instability located on the dithiolate stacks to the lattice via a stack dimerization.

### a- Spin-Peierls structural fluctuations

The SP instability of the M = Ni, Pd and Pt dithiolate stacks is detected by the observation of a sizeable regime of 1D diffuse structural fluctuations appearing as diffuse lines located in b*/2 on X-ray diffuse patterns. Such diffuse lines have been observed in the Pt ([9] – see also figure 5a), Ni [21] and Pd [9] derivatives. The reduced critical wave vector of the fluctuations $q_{SP}$=b*/2 corresponds to an incipient instability towards a dimerization of the dithiolate stack. This dimerization should lead to a pairing of neighbouring S=1/2 spins into a singlet.

These diffuse lines have been detected below 30K, 100K and 100K in the Pt, Ni and Pd salts respectively. This onset temperature, given in table II, is taken as the SP mean-field temperature ($T_{SP}^{MF}$) of the dithiolate stacks. $T_{SP}^{MF}$ is twice larger than the temperature at which Peierls fluctuations begin to manifest (i.e. temperature of the minimum of electrical resistivity, $T_\rho$, see table II). This is a clear experimental evidence that the SP instability on dithiolate stacks starts before the Peierls instability on Per stacks.

Preprints (www.preprints.org) | NOT PEER-REVIEWED | Posted: 26 January 2017 doi:10.20944/preprints201701.0118.v1

Peer-reviewed version available at Magnetochemistry 2017, 3, 13; doi:10.3390/magnetochemistry3010013



| $Per_2[M(mnt)_2]$ | $T_P/T_{SP}$ (K) | b*/4 Peierls modulation | b*/2 spin-Peierls modulation | $T_\rho$ (K) | 1D SP fluctuations |
|---|---|---|---|---|---|
| M=Pt | 8.2/"7.5" | not observed | SRO in all directions | 18 | ≤ 30K |
| M=Ni | 25/"25-45" | LRO | SRO in all directions | 50 | ≤ 100K |
| M=Pd | 28/28 | not observed | LRO | 50-80 | ≤ 100K |

Table II. Characteristics of α-$Per_2[M(mnt)_2]$ salts exhibiting both a Peierls and a spin-Peierls instability for M=Pt, Ni and Pd. The metal-insulator Peierls transition temperature ($T_P$) and the temperature of minimum of resistivity ($T_\rho$) are taken from electrical measurements of ref. [7, 8]. The SP critical temperature and the nature of the short range (SRO) or long range (LRO) SP order detected below $T_{SP}$ are indicated as well as the temperature range of observation of 1D SP fluctuations. "$T_{SP}$" values given for the Ni and Pd derivatives are the temperature at which the extrapolation of the quantities $\chi_{SP}^{-1}(q_{SP})$ and $\xi_b^{-1}$ deduced from 1D SP fluctuations and plotted in figures 6 and 7, vanish.

The SP structural fluctuation can be quantitatively analyzed from the thermal dependence of the intensity and profile of the diffuse lines along the chain direction b [9], namely:

- the $q_{SP}$ peak intensity $I(q_{SP})$ or more likely the $T/I(q_{SP})$ ratio which is proportional to the inverse of the SP structural susceptibility $\chi_{SP}^{-1}(q_{SP})$ (see figure 6).
- the half width at half maximum (corrected by the experimental resolution) which give the inverse coherence length of the SP fluctuation in chain direction $\xi_b^{-1}$ (see figure 7).

$\chi_{SP}(q_{SP})$ exhibits a Curie-Weiss like divergence for the Pd and Pt salts as predicted for the high temperature fluctuations of the amplitude of the order parameter (i.e. regime of Gaussian fluctuations) [34]. The linear dependence of the inverse susceptibility shown in figure 6:

$$\chi_{SP}^{-1}(q_{SP}) \propto (T - T_{SP}), \quad (5)$$

allows to define a $T_{SP}$ at about 28K and 7.5K for the Pd and Pt salts. For the Ni salt $\chi_{SP}^{-1}(q_{SP})$ does not really vanishes upon cooling. Figure 6 shows that the high temperature data extrapolate linearly to a "$T_{SP}$" of about 25K.

The correlation length increases in an inverse square root law as predicted in the regime of Gaussian fluctuations of the amplitude of the order parameter [34]. The square root thermal dependence of the inverse correlation length is shown in figure 7:

$$\xi_b^{-1} \propto \sqrt{(T - T_{SP})} \quad . \quad (6)$$

The extrapolation at zero of expression (6) leads to the same $T_{SP}$ as does expression (5) for the Pd and Pt salts.

For the Pd salt, $\chi_{SP}(q_{SP})^{-1}$ and $\xi_b^{-1}$ vanish at $T_{SP}$=28K. Below this $T_{SP}$ SP superstructure reflections are detected at the reciprocal wave vector $q_{SP}$=b*/2 [9]. There is thus below $T_{SP}$ a long range SP order. The Pd salts exhibits all the structural characteristics of a well-defined 2nd order SP transition.

Preprints (www.preprints.org) | NOT PEER-REVIEWED | Posted: 26 January 2017 doi:10.20944/preprints201701.0118.v1

Peer-reviewed version available at Magnetochemistry 2017, 3, 13; doi:10.3390/magnetochemistry3010013



$\chi_{SP}(q_{SP})^{-1}$ and $\xi_b^{-1}$ measured in the Pt salt tend to vanish at about 7.5K. However the X-ray pattern taken at 4K (figure 5b) shows that only a SP SRO is achieved. There is thus a pseudo-SP transition at a "$T_{SP}$ "≈7.5K in table II.
No vanishing of $\chi_{SP}(q_{SP})^{-1}$ and $\xi_b^{-1}$ is found for the Ni salt. $\xi_b^{-1}$ saturates below 50K while the high temperature data extrapolates to zero around 45K. $\chi_{SP}^{-1}(q_{SP})$ changes of slope below 35K while the high temperature data linearly extrapolates to zero around 45K. These two "$T_{SP}$" values of extrapolation are indicated in table II.

### b- Spin-Peierls and Peierls orders

Table II gives the Peierls critical temperature (on Per stack) deduced from the metal to insulator transition detected by conductivity measurements [7, 8]. Very weak $2k_F^D=b^*/4$ super-lattice reflections have been detected below $T_P$ in the Ni salt [21]. They have an intensity comparable to those found below $T_P$ in the Cu derivative. No b*/4 super-lattice reflections have been detected in the Pd and Pt derivatives. They could be too weak to be detected especially in the Pt derivative.

$T_{SP}$ and "$T_{SP}$" values reported in table II are the temperature at which 1D SP fluctuations diverges or tends to diverge as discussed above in part a. Sharp b*/2 SP superstructure reflections are observed below $T_{SP}$=28K in the Pd salt [9].
"$T_{SP}$" is a pseudo SP transition temperature for the Ni salt since the low temperature saturation of $\chi_{SP}(q_{SP})^{-1}$ and $\xi_b^{-1}$ reveals a short range dimerization order in all the spatial directions [21]. At 9K the SP dimerization extends on 35Å (8b) in stack direction and the SP phasing extend only on 14Å in lateral direction. This last distance corresponds to the distance between first neigboring dithiolate stacks. In this respect the transverse interaction between first neighbor dithiolate stacks should be mediated through a perylene stack (see figure 2). Such a coupling should be weak, which explains why dimerization of only first neighbor dithiolate stacks are correlated in the SP ground state. Note that in the Ni derivative such a SP SRO cannot be ascribed to disorder in the material because sharp b*/4 superstructure reflections are observed (note also that a similar SP SRO is observed in the Pt derivative – see below).
A somewhat similar situation is observed in the Pt derivative. A specific heat anomaly indicates the occurrence of a thermodynamic phase transition around 8K [35]. However table II indicates a $T_P$ (8.2K: metal-insulator transition from transport measurements) distinct from "$T_{SP}$" (7.5K: temperature at which 1D SP fluctuations tend to diverge). Note that in agreement with the finding of a structural "$T_{SP}$" the abrupt drop of the EPR signal below 7.5K indicates a concomitant loss of spin degrees of freedom [36]. The finding of a $T_{SP}$ distinct from $T_P$ seems to be sustained by extrapolation to 0K of the magnetic phase diagram [37].
The establishment of a low temperature spin-singlet ground state on $[Pt(mnt)_2]$ chains is evident from $^1$H NMR spectra and spin relaxation ($1/T_1$) rates [38, 39]. However NMR cannot probe the spatial extend of the SP order. Thus a possible explanation of the decoupling between $T_P$ and "$T_{SP}$" could rely on the observation that the SP order remains incomplete. The X-ray pattern shown in figure 5b proves that there is not a long range SP dimerization at 4K: the SP dimerization extends on 36Å (9b) in stack direction and 16Å (i.e. the first neighbor dithiolate distance) in transverse direction. Note that these correlation lengths are comparable to those found in the Ni derivative. This means that only a short range SP phasing occurs both in longitudinal and transverse directions. An incomplete SP pairing means that unpaired spins 1/2 should remain present. A minority of such spins has been recently identified by low

temperature NMR measurements [39]. Note that the presence of low temperature unpaired spins agrees with the observation of a finite 0K spin susceptibility in the Pt salt [38, 39].
The simultaneous presence of incomplete transverse and longitudinal SP orders and of unpaired spins ½ can be rationalized in a unified description using a previous interpretation of similar findings in doped $CuGeO_3$ SP systems [40]. In the SP ground state the minimum of inter-chain coupling energy generally imposes an out of phase transverse phasing between dimerization on first neigbouring chains (this corresponds to a minimum of Coulomb coupling between such charged chains). This minimum of energy implies that dimerization are shifted by b between first neighboring chains. Within such a SP pattern the staggered transverse order can be easily broken by keeping the dimerization of two neighboring chains in phase. The defect consists in an absence of relative shift of dimerization between two first neighbor chains. Thus with respect to the staggered transverse dimerization order such a linear defect introduces a relative transverse phase shift of π between SP patterns on left and right sides of the defect. This defect cost locally a maximum of inter-chain coupling energy. In that situation the best way to limit the cost of coupling energy between two chains having the wrong relative phasing is to reduce the spatial extent of the linear defect by restoring the out of phase inter-chain dimerization order. This can be achieved by limiting the extent of the defect by leaving unpaired two spins ½ on each side if the linear defect. Each unpaired spin introduces a defect of dimerization which changes by ±π the phase of the intra-chain structural modulation. The creation of pairs of ±π dimerization defects thus limits the spatial extend of the longitudinal SP order (the average distance between the two dimerization defects being of the order of $\xi_b$). As each dimerization defect bears an unpaired spin ½, the limitation of the SP order in chain direction causes the presence of S=1/2 free spins. These magnetic defects have been observed in the SP ground state of the Pt derivative. In our description the limitation of the longitudinal order is caused by the break of the transverse order, but the reverse is also true. Unpaired spins are created by any type of defect interrupting the SP longitudinal order.

### c- Mechanism of the SP instability in α-$(Per)_2[M(mnt)_2]$

Table II gives the temperature at which 1D SP fluctuations begin to be detected. This temperature is taken as the mean-field temperature of the SP transition $T_{SP}^{MF}$ [34]. One thus has $T_{SP}^{MF} \approx 30K$ for the Pt salts and 100K for the Pd and Ni salts. $T_{SP}^{MF}$ is related to the mean field SP gap, $\Delta^{MF}$, by the mean-field correspondence relationship, which can be expressed for the Heisenberg chain by [41]:

$$\Delta^{MF} \approx 2.47 k_B T_{SP}^{MF} \quad (7)$$

With the above quoted $T_{SP}^{MF}$ values one gets $\Delta^{MF} \approx 75K$ for the Pt salts and 250K for the Pd and Ni salts.
In this framework the nature of the SP ground state depends on the relative value of the mean-field gap $\Delta^{MF}$ with respect to the critical phonon energy at $q_{SP}$: $\hbar\Omega_C \approx 50\text{-}100K$ for TA-LA phonon frequencies in organics [42]. For the 0K Heisenberg chain, the SP transition occurs in the classical (adiabatic) limit when $\hbar\Omega_C \leq \Delta^{MF}/2$ [43]. In the opposite limit of weak $\Delta^{MF}$, $\hbar\Omega_C \geq \Delta^{MF}/2$, the SP transition occurs in the quantum (anti-adiabatic) limit. Note that if $\Delta^{MF}$ is small enough such that $\Delta^{MF} \leq 0.7\hbar\Omega_C$ [44], the zero point phonon quantum fluctuations kills the SP dimerization. In that case the SP gap vanishes exponentially at a quantum critical point beyond which a spin liquid state is stabilized. The 0K phase diagram of the SP ground state of the AF Heisenberg chain is shown in figure 8. This figure shows that the SP transition of Pd and Ni salts occurs in the adiabatic limit while the SP transition of the Pt salt occurs in the non-adiabatic limit.

Preprints (www.preprints.org) | NOT PEER-REVIEWED | Posted: 26 January 2017 doi:10.20944/preprints201701.0118.v1

Peer-reviewed version available at Magnetochemistry 2017, 3, 13; doi:10.3390/magnetochemistry3010013



In the adiabatic limit, when the dynamics of SP structural fluctuations is slow compared to those of magnetic degrees of freedom, the local SP pairing, which develops below $T_{SP}^{MF}$, progressively forms a pseudo-gap in the density of states of magnetic excitations, which manifests by a depression of spin susceptibility. In the opposite anti-adiabatic limit, the dynamics of SP structural fluctuations is so rapid that the spin susceptibility remains unaffected in the fluctuation regime. A typical example of adiabatic SP transition is the (BCP-TTF)$_2$X series and of anti-adiabatic SP transition is MEM-TCNQ [45, 34, 2, 3]. Additional examples are given in figure 8.

In order to analyze the influence of the SP instability on the spin degrees of freedom let us first consider the spin susceptibility, $\chi_S$, of the Pd, Ni and Pt salts shown in figure 9a [8]. In a first approximation, the dithiolate stacks can be described by a collection of isolated S=1/2 AF chains. Then each magnetic chain can be modeled by the simplest Heisenberg Hamiltonian:

$$H_{dith.} = J_1 \sum_j \boldsymbol{S}_j \boldsymbol{S}_{j+1}, \quad (8)$$

where $J_1$ is the first neighbor exchange interaction. With this Hamiltonian the thermal dependence and the magnitude of the spin susceptibility $\chi_S(T)$ can be exactly calculated [46]. Using this simplest description figure 9b gives at each temperature for the Pd, Ni and Pt salts the effective first neighbor exchange interaction $J_{1eff}$ taken from the absolute value of the spin susceptibility [47]. This figure shows in particular that:

- in the Pd salt $J_{1eff}$ saturates at 260K above 100K,
- in the Pt salt $J_{1eff}$ saturates at 35K below 90K,
- in the Ni salt $J_{1eff}$ increases linearly between 300 and 100K.

Figure 9b shows in certain temperature ranges deviations at these simple dependences. This means that the above description must be completed by adding other terms in the Hamiltonian (8). Below we consider coupling with SP structural fluctuations (as already done in ref.[34]) and exchange coupling with conduction electron spins on Per stacks (as already done in ref.[38]).

Let us start with the SP instability of the Pd salt which occurs in the adiabatic limit. Let us also remark that relevant energies of its SP instability ($J_1 \approx 260$K and $T_{SP}^{MF} \approx 100$K) are comparable to those of the (BCP-TTF)$_2$X series ($J_1 \approx 270$K, $T_{SP}^{MF} \approx 120$K for X=$AsF_6$ and $J_1 \approx 330$K, $T_{SP}^{MF} \approx 100$K for X=$PF_6$ [45]). One also have for these organic compounds similar critical phonon frequencies, $\Omega_C$. Figure 9a shows that the spin susceptibility of the Pd salt behaves above 100K as $\chi_S$ of an S=1/2 AF chain with $J_1 \approx 260$K. Below $T_{SP}^{MF} \approx 100$K SP lattice fluctuations develop on a correlation length $\xi_b$ (whose inverse length is given in figure 7) a local spin singlet S=0 state. This local singlet non-magnetic order induces below 100K a pseudo-gap in the magnetic excitation spectrum which manifests (see figure 9a) by a decrease of the spin susceptibility with respect to $\chi_S$ of the uniform 1D AF chain. This feature is also revealed by a net increases of $J_{1eff}$ below 100K (see figure 9b). This thermal behavior, which resembles to the one measured in (BCP-TTF)$_2$X salts, can be quantitatively accounted for by the coupling of AF fluctuations to SP critical lattice fluctuations [34]. The drop of $\chi_S$ is quantitatively similar in the Pd derivative and in (BCP-TTF)$_2$X between 100K and 50K. Below 50K $\chi_S$ of the Pd salt drops abruptly to nearly vanishes at $T_{SP}$=28K (figure 9a), while $\chi_S$ of (BCP-TTF)$_2$X SP continues to decrease monotonously and remains finite at its SP transition [45, 34]. Thus the vanishing of $\chi_S$ below 50K in the Pd derivative cannot be due to SP structural fluctuations which diverge continuously in temperature (figures 6 and 7) as those measured in (BCP-TTF)$_2$X [45, 34].

Preprints (www.preprints.org) | NOT PEER-REVIEWED | Posted: 26 January 2017 doi:10.20944/preprints201701.0118.v1

Peer-reviewed version available at Magnetochemistry 2017, 3, 13; doi:10.3390/magnetochemistry3010013



In order to account for the abrupt vanishing of $\chi_S$ observed below 50K in the Pd derivative one has to consider thermal dependent modification of magnetic exchange interactions on dithiolate stacks. Below we propose that such a modification arises from the AF exchange coupling between the localized spins $\boldsymbol{S}_j$ on dithiolate molecules "j" and the spin density $\boldsymbol{s}_l(x)$ on neighboring "*l*" metallic Per chains. Since the net decrease of $\chi_S$ coincides with the development of a $2k_F$ density wave instability on the Per stack (which should grow below about $T_\rho \approx$50-80K – see table II) the inter-stack coupling appears to be pertinent below a quite well defined temperature, noted $T_{per.coupl.}$ in figure 9a, close to $T_\rho$. Below $T_{per.coupl.}$ the $2k_F$ electron-hole instability on the Per stack, $\chi_{eh}(2k_F^D, T)$, submitted to an "external" AF field originating from the localized spins on dithiolate stacks responds by setting a $2k_F$ spin density wave (SDW) $\boldsymbol{s}_l(x)$, as schematically illustrated by figure 10.

Following the notations of ref. [38], this additional interaction can be modeled by adding to the direct exchange Hamiltonian (8) an inter-chain exchange coupling Hamiltonian involving the spins density $\boldsymbol{s}_l(x)$ located on neighboring Per sacks:

$$H_{coupl.} = \sum_{l,per.} \int \left[ H_l^{1D\ cond}(x) + J_\perp \sum_{j,dith.} \boldsymbol{S}_j\, \boldsymbol{s}_l(x) \right] dx \quad (9)$$

The first term of the right member of expression (9) $H_l^{1D\ cond}(x)$ is the Hamiltonian of the 1D conduction electron gas located on Per stacks "*l*"; x being the stack direction. In the second term $J_\perp$ is the transverse AF exchange coupling between nearest dithiolate and per spins, respectively $\boldsymbol{S}_j$ and $\boldsymbol{s}_l(x)$. Note, as shown in figure 2, that there are three different types of $J_\perp$ interactions per Per (the strongest one should occur in the direction of maximum overlap of dithiolate and per molecular orbitals). Experimental evidence for a sizeable transverse exchange coupling, $J_\perp$ (or for a fast inter-chain spin exchange regime) is provided by the observation for Pd [48] and Pt [38] derivatives of a single EPR line at a g value intermediate between those of $[M(mnt)_2]$ and Per molecules.

Due to the 1D nature of its electron gas, the Per stack exhibits a divergent electron-hole response $\chi_{eh}(q, T)$ which sizably increase below $T_\rho$ for $q=2k_F^D= b^*/4$. In this regime a spin $\mathbf{S}^0$ located on a dithiolate molecule placed at the origin should polarize through the AF exchange coupling $J_\perp$ the electronic spins $\boldsymbol{s}_l(\boldsymbol{x})$ located on neighboring per stacks (figure 10). This induces a SDW s(x) on Per stacks whose thermal and spatial dependences are given by the 1D Fourier transform of $\chi_{eh}(q)$ (assumed here to be that of a free electron gas):

$$s(x) \sim \chi_{eh}(2k_F^D, T) \frac{\cos(2k_F^D x)}{x} e^{-x/\xi_T} \quad (10)$$

In (10) the SDW which oscillates with the period 4b is also damped by the thermal electronic length $\xi_T$ issued from the thermal broadening of the FS. At a distance x=mb from the origin the oscillating spin density s(x) exhibits, through $J_\perp$, a modulated magnetic coupling with the spin $S^m$ located on the near neighbor dithiolate molecules "m". Through the spin polarization of Per stack, this induces a spatially dependent effective exchange coupling between spins $\mathbf{S^0}$ and $\mathbf{S^m}$ distant of mb on the same dithiolate stack. Such an indirect oscillating interaction is known in the literature as the Rudernann-Kittel-Kasuya-Yosida (RKKY) interaction. It behaves basically in 1D as [49]:

$$J_{RKKY}^m(2k_F^D, T) \sim -|J_\perp|^2 \chi_{eh}(2k_F^D, T) \frac{\cos(m\pi/2)}{m} e^{-mb/\xi_T} \quad (11)$$

The mediated interaction (11) provides in particular an indirect AF coupling between spins located on every second molecules (m=2) on the dithiolate stack. As shown in figure 10 this indirect AF coupling competes with the intra-stack second neighbor effective ferromagnetic

Peer-reviewed version available at Magnetochemistry 2017, 3, 13; doi:10.3390/magnetochemistry3010013



coupling due to the succession of two first-neighbor direct AF interaction $J_1$. Furthermore because of the 1D nature of the electron gas on Per stack $\chi_{eh}(2k_F^D, T)$ sizably increases upon cooling (with a logarithmic thermal divergence for a 1D free electron gas). Thus the amplitude of the second neighbor AF interaction $J_{RKKY}^{m=2}(2k_F^D, T)$ grows with respect to $J_1$ when T decreases.

1D magnetic chain with first, $J_1$, and second, $J_2$, neighbor frustrated AF interactions presents a very unusual phase diagram at 0K (see for example [51]). When the ratio of exchange coupling $\alpha = J_2/J_1$ is smaller than $\alpha_c \approx 0.24$, the ground state is a gapless spin fluid state, with a quasi-long range AF order. This ground state changes when $\alpha \geq \alpha_c$, through a quantum critical point located at $\alpha_c$, into a gapped state with long range dimer order. Note that when the ratio of exchange coupling $\alpha$ is larger than $\alpha_c$ a singlet-triplet spin gap opens in absence of any coupling with the phonon field. In the Pd salt, the rapid vanishing of the spin susceptibility observed below 50K (figure 9a) could be caused by the rapid growth of the ratio of exchange coupling $\alpha$ due to the thermal increase of $J_{RKKY}^{m=2}(2k_F^D, T)$ below $T_\rho$. However as SP critical fluctuations continue to diverge upon cooling the total singlet-triplet gap should superimpose the effects of the SP lattice dimerization and of the frustration of AF coupling. Such combined effects have been considered in the literature [52, 53].

The SP instability of the Ni salt occurs also in the adiabatic limit. There are however some differences between the Ni and Pd salts. The most important difference is that $J_{1eff}$ increases linearly when T decreases between 300 and 100K (figure 9b), while $J_{1eff}$ was constant in the same temperature range for the Pd salt. It is thus possible that the increase of $J_{1eff}$ results from an increase of the intra-stack overlap between dithiolate MO upon cooling due a continuous sliding of neighboring Ni(dmit)$_2$ molecules. However there is a clear deviation at the linear increases of $J_{1eff}$ below 100K when SP structural fluctuations develops. This could be due, as for the Pd salt, to the growth of a pseudo-gap in the AF magnetic excitation spectrum. Also similarly to the Pd salt, $\chi_S$ abruptly drops below 50K and vanishes around 20K (figure 9a). Note however that if below 50K $\chi_S$ exhibits the same temperature dependence for the two salts, figures 6 and 7 show that SP structural fluctuations behave differently for the Ni and Pd derivatives in that temperature range. While SP fluctuations diverge at $T_{SP}$=28K in the Pd derivative, SP fluctuations reduce their divergence below ~50K (for $\xi_b$) and ~35K (for $\chi_{SP}$) in the Ni derivative. Thus the rapid decrease of $\chi_S$ in the Ni derivative cannot be due to the critical growth of SP fluctuations. As $\chi_S$ considerably decreases below $T_\rho \approx 50$K when $\chi_{eh}(2k_F^D, T)$ sizably increases, the spin gap opening is more likely due to a frustration effect between second neighbor indirect $J_{RKKY}^{m=2}(2k_F^D, T)$ and first neighbor direct $J_1$ AF interactions on the Ni dithiolate stack.

Figure 9a shows that the thermal dependence of $\chi_S$ below ~40K resembles that of a thermally activated excitation process. For an activated process through a gap $\Delta$, the spin susceptibility of a classical assembly of spin ½ behave as:

$$\chi_s(T) \propto \frac{1}{T} e^{-\Delta/T} \qquad (12)$$

Data of figure 9a give $\Delta \sim 130$K, which amount to about $J_1/2$. We thus propose that the gap which develops below 50K is a singlet triplet gap set by frustration effects between first and second neighbor AF interactions when $\alpha = J_1/J_2 \geq \alpha_c \approx 0.24$. Note that the opening of a gap $\Delta \sim J_1/2$ in absence of sizeable lattice dimerization requires sizeable AF frustration effects with $\alpha \sim 0.5$ [53]. $\alpha = 0.5$ corresponds to the so-called Majumdar-Ghosh point where the ground

state of the AF chain, which corresponds to two possible dimerization patterns formed by a succession of disconnected singlet dimers, is twofold degenerate.

The magnetic properties of Pt salt have been already considered in ref. [38] suggesting the presence of mediated RKKY interactions through the Per stack. However the physics of Pt salt differs on many aspects from the one exhibited by the Pd and Ni salts. Firstly the SP instability of the Pt salt occurs in the non-adiabatic limit. Thus the development of structural SP fluctuations below 30K ($T_{SP}^{MF}$) should not create a pseudo-gap in the spin excitations. Accordingly the thermal dependence of the $\chi_S$ should not deviate appreciably between $T_{SP}^{MF}$ and $T_{SP}$ from the extrapolated high temperature dependence of $\chi_S$ (more precisely figure 9b shows that $J_{1eff}$ should not change appreciably below 30K). A similar behavior is shown by $\chi_S$ in the non-adiabatic SP compound MEM-$(TCNQ)_2$ [45, 2, 3]. Secondly SP fluctuations start below 30K in the temperature range where the AF correlations are not developed (AF correlations develop when $\chi_S$ begins to decrease below ≈20K,). The nature of the driving force of the SP instability in the Pt salt is thus questioned because the SP instability, being triggered by quantum fluctuations of the AF chain, should start only in presence of AF correlations (i.e. in the temperature range below the maximum of $\chi_S$).
All these features require a clarification of the various types of effective spin-spin interactions occurring on the Pt dithiolate stack. In particular and in addition to the first neighbor AF interaction $J_1$ (estimated at ~35K from the fit of $\chi_S$ by the contribution (8) – see figure 9b) additional AF interactions which competes with $J_1$ should be considered. Firstly one expects to have below $T_\rho$≈18K, when the electron-hole response of the Per stack develops a second neighbor mediated AF interaction $J_{RKKY}^{m=2}(2k_F^D, T)$ as for the Pd and Ni derivatives. Secondly the SP magneto-elastic coupling leads in the non-adiabatic regime to a renormalization of $J_1$ and induces a second neighbor AF interaction $J_2$ [44]. For these two reasons the spin-spin Hamiltonian of the dithiolate stack should include first and second neighbor AF competing interactions. However as $\chi_S$ does not decrease drastically on approaching $T_{SP}$, the frustration ratio $\alpha=J_1/J_2$ should remain small (less than $\alpha_c$?), at the difference of Pd and Ni derivatives. Nevertheless in presence of these additional effects $\chi_S$ of the Pt salt should behave differently as predicted by the simple $J_1$ Hamiltonian (8).

### d- Nature of the ground state

In the previous section we have shown, especially for the Pd and Ni derivatives that $Per_2[M(mnt)_2]$ salts exhibit magnetic properties on dithiolate stacks coupled to a $2k_F$ density wave instability of the conducting Per stacks. Such features place $Per_2[M(mnt)_2]$ among Kondo lattices where magnetic properties of localized spins are coupled to itinerant spins of the conduction electron gas. Furthermore the 1D nature of both the transfer integrals in the metallic subsystem and of the $J_1$ AF exchange coupling in the magnetic subsystem locate $Per_2[M(mnt)_2]$ among the 1D two chain Kondo lattices since, as shown in figure 2, magnetic chains are spatially decoupled from the conducting chains. There is an abundant literature on 1D Kondo lattices involving elaborated theoretical considerations [51, 54]. However experimental clear-cut evidence of 1D Kondo lattices are quite sparse in the literature. Following our interpretation of experimental data, it seems that $Per_2[M(mnt)_2]$ organic salts with M=Ni and Pd are a good realization of 1D Kondo lattice physics; this is less clear for the Pt derivative.
In this framework it has been proposed that spin dimerization observed in $Per_2[M(mnt)_2]$ salts could be explained using a 1D Kondo lattice model at quarter filling with some kind of

RKKY interaction between localized moments [55]. However the realization of such a ground state is not obvious because it has been numerically shown that a frustrated spin-1/2 Heisenberg chain coupled to adiabatic phonons can exhibit a tetramerized phase for a large enough frustration ratio α and a large spin-lattice coupling [56]. These different theoretical finding show that the physics of $Per_2[M(mnt)_2]$ should be quite subtle because there are two competing periodicity in the system: $2k_F^D=b^*/4$ for the ¨Peierls instability on the Per stack and $2k_F^{SP}=b^*/2$ for the SP instability on the dithiolate stack.

In presence of non-magnetic dithiolate stacks the Peierls transition stabilizes the $2k_F^D$ modulation as shown by experimental studies of M=Cu, Co and Fe compounds (table I). Complications arise in salts where with M=Ni, Pd and Pt the dithiolate stack is magnetic and where, with a sizeable magneto-elastic coupling, a SP instability develops at $2k_F^{SP}$, which is two times $2k_F^D$. In Ni, Pd and Pt salts there is no experimental evidence that both $2k_F^D$ and $2k_F^{SP}$ LRO are simultaneously stabilized at low temperature. In the Ni derivative where frustration effects are more apparent there is below 25K a $2k_F^D$ LRO and a $2k_F^{SP}$ SRO. It is thus possible that the b*/2 SP divergence on the dithiolate stacks stops around 50-35K when the sizably frustrated spin system (α~0.5) is quite strongly coupled to an adiabatic phonon field. In that case the system should prefer to be tetramerized as predicted in ref. [56]. In $Per_2[Ni(mnt)_2]$ the $2k_F^D$ LRO was initially attributed to the Peierls modulation on the Per stack. However one cannot exclude that a component of such a modulation should originate from the $Ni(dmit)_2$ stacks. In the Pd derivative the situation is different because a $2k_F^{SP}$ LRO is detected without any evidence of a $2k_F^D$ Peierls order; a feature which remains to be explained. In the Pt derivative there is a short range SP order in all the directions (of spatial extend comparable to the one of the Ni derivative) but figure 5b does not provide any evidence of a $2k_F^D=b^*/4$ Peierls modulation. However such a Peierls modulation could be too weak to be detected because the Peierls gap is quite small (one expects from the relative magnitude of the Peierls gap super-lattice reflections 3 times less intense in the Pt salt than those detected in the Ni salt). Note however that the existence of a CDW modulation in the Pt derivative is assessed by the observations of non-linear conductivity effect due to the sliding of CDWs under electric field [23].

A key parameter of control of the phase diagram of $Per_2[M(mnt)_2]$ relies on the presence of a sizeable inter-stack coupling. A close inspection of the structure shown in figure 2 shows that if there are many direct interactions between Per stacks [10] the interaction between dithiolate stacks should be mediated through Per stacks. Thus if Per stacks are the source of RKKY mediated interactions between localized spins on dithiolate stacks one expects the presence of induced $2k_F^D$ SDW fluctuations on Per stacks (figure 10). Such SDW fluctuations should compete with $2k_F^D$ BOW/CDW fluctuations at the origin of the Peierls instability. Up to now there is no evidence of such a magnetic instability on the Per stack. However it is possible that the modulation of Per stacks below $T_P$ should be a mixed $2k_F^D$ SDW-CDW as found in the magnetic ground state of $(TMTSF)_2PF_6$ [57, 58]. This could arise in the Pd derivative where standard $2k_F^D$ Peierls superstructure reflections have not been detected.

Also in order to establish the RKKY mediated interaction the $2k_F^D$ electron-hole instability on the Per stack is of fundamental importance since it tunes the magnitude of the indirect AF coupling interaction via the thermal divergence of the electron-hole response function below $T_\rho$. As the Peierls instability starts on Per stacks below $T_\rho$, which occurs below $T_{SP}^{MF}$, one observes on Ni and Pd dithiolate stacks first a SP instability then, below about $T_\rho$, a vanishing of the singlet-triplet gap due to the growth of frustrated 2nd neighbor AF interactions. If the $2k_F^D$ electron-hole instability was sizably stronger, as for example in the $(arene)_2 PF_6/AsF_6$

salts, the AF frustration will be set before the start of the SP instability. Thus with the opening of a high temperature singlet-triplet gap due to AF frustration, the driving force for the SP instability could not be activated. These features show that the original magnetic phase diagram of dithiolate stacks results from a fine tuning with the Peierls instability on Per stacks.

To finish, note that α-$Per_2[M(mnt)_2]$ is a representative example of two-chain 1D Kondo lattices where magnetic chains are spatially decoupled from conducting chains; both kinds of chain being of different chemical nature (anion/donor). This is different from standard one chain Kondo lattices where, because of the involvement of different orbital degrees of freedom in the vicinity of the Fermi level, spin localized electrons and conducting electrons belong to the same chain. This is the case of the inorganic 1D conductor $BaVS_3$ where each V atom shares one average one-half delocalized $d_{z^2}$ electron, which partly fill a 1D conduction band, and one-half localized e($t_{2g}$) electron of spin ½ [59]. Because of the coupling between the two electron species $BaVS_3$ exhibits a quite subtle low temperature magnetic structure where the nodes of the S=1/2 AF modulation are occupied by spin singlet pairs issued from the Peierls distortion of the $d_{z^2}$ 1D electron gas [60].

## IV- Conclusion

In this paper we have reviewed the structural properties of the α-$Per_2[M(mnt)_2]$ series of organic conductors. When the dithiolate stack is diamagnetic for M=Au or Cu or strongly dimerized for M=Co and Fe, the Per stack undergoes a $2k_F^D=b^*/4$ Peierls instability. However the Peierls transition occurs at temperatures, $T_P$~12-73K, more than twice smaller than those $T_P$~160-180K found in other quarter-filled $D_2X$ arene cation radical salts where D is either FA or substituted Per and X is a monovalent anion such as $PF_6$ and $AsF_6$. In the case of 1D S=1/2 AF dithiolate stack for M=Ni, Pd and Pt a SP instability develops at $2k_F^{SP}=b^*/2$. As this last wave vector is twice larger than $2k_F^D$, very rich ground states are observed in these salts. The SP instability of the Ni and Pd derivatives occurs in the classical limit with the formation of a pseudo-gap, in the AF magnetic excitations spectrum, driven by the growth of structural SP fluctuations below 100K. Surprisingly the spin susceptibility of these salts drops below 50K to finally vanish around 20K. We attribute this unexpected behavior to the growth of a singlet-triplet gap caused by frustration of S=1/2 AF interactions on dithiolate stacks. Frustration is attributed to the presence of a second neighbor indirect RKKY S=1/2 AF interaction mediated by a fine tuning with the $2k_F^D$ electron-hole instability of the Per stack. This subtle coupling between magnetic and conducting chains shows that the family of α-$Per_2[M(mnt)_2]$ compounds provides for Ni and Pd a remarkable realization of 1D Kondo lattices. A somewhat different magnetic behavior, with no so clear cut manifestation of the 1D Kondo lattice coupling, is observed in the Pt derivative whose SP instability occurs in the quantum limit.

**Acknowledgments**

Earlier structural studies reported in this review have been performed by V. Gama, R.T. Henriques, V. Ilakovac and S. Ravy. One of us (JPP) recognizes very fruitful discussions with C. Bourbonnais.

[1] Comès R., Lambert M., Launois H. and Zeller H.R. Evidence for a Peierls Distortion or a Kohn Anomaly in One-Dimensional Conductors of the Type $K_2Pt(CN)_4Br_{0.30}.xH_2O$. *Phys. Rev. B* **1973**, 8, 571-575.

[2] Pouget J.-P. Bond and charge ordering in low-dimensional organic conductors. *Physica B* **2012**, 407, 1762–1770.

[3] Pouget J.-P. The Peierls instability and charge density wave in one-dimensional electronic conductors. *C. R. Physique* **2016**, 17, 332–356.

[4] Schlenker C., Dumas J., Greenblatt M. and van Smaalen S. (Eds). Physics and Chemistry of Low-Dimensional Inorganic Conductors. *Nato ASI Series B: Physics* (Plemum Press, New-York 1996) Vol. 354.

[5] Pouget J.-P. Interplay between electronic and structural degrees of freedom in quarter-filled low dimensional conductors. *Physica B* **2015**, 460, 45–52.

[6] Akamatsu A., Inokuchi H. and Matsunaga Y., Electrical Conductivity of the Perylene-Bromine Complex. *Nature* **1954**, 173, 168-169.

[7] Almeida M. and Henriques R.T. Perylene Based Conductors, chapter 2 in *Handbook of Organic Conductive Molecules and Polymers Volume 1 "Charge Transfer Salts, Fullerenes and Photoconductors"* Edited by Nalva H.S. (John Wiley & Sons Ltd, 1997), pp 87-149.

[8] Gama V., Henriques R.T., Bonfait G., Almeida M., Ravy S., J.P. Pouget and Alcacer L. The interplay between conduction electrons and chains of localized spins in the molecular metals $(Per)_2M(mnt)_2$, M=Au, Pt, Pd, Ni, Cu, Co and Fe.*Mol. Cryst. Liq. Cryst.* **1993**, 234, 171-178.

[9] Henriques R.T, Alcacer L., Pouget J.P. and Jérome D. Electrical conductivity and x-ray diffuse scattering study of the family of organic conductors $(perylene)_2M(mnt)_2$, (M=Pt, Pd, Au). *J. Phys. C: Solid State Phys*. **1984**, 17, 5197-5208.

[10] Canadell E., Almeida, M. and Brook J. Electronic band structure of α-$(Per)_2M(mnt)_2$ compounds. *Eur. Phys. J. B* **2004**, 42, R453.

[11] Monchi K., Poirier M., Bourbonnais C., Matos M.J. and Henriques R. T. The Peierls transition in $Per_2$ $[Au_xPt_{1-x}(mnt)_2]$: pair-breaking field effects. *Synth. Met.* **1999**,103, 2228-2231.

[12] (a) Almeida M., Gama V., Santos I.C., Graf D. and Brooks J.S. Counterion dimerisation effects in the two-chain compound $(Per)_2[Co(mnt)_2]$: structure and anomalous pressure dependence of the electrical transport properties. *CrystEngComm* **2009**, 11, 1103–1108. (b) Santos I.C., Gama V., Silva R.A.L. and Almeda M. unpublished result.

[13] Ilakovac V., Ravy S., Pouget J.P., Riess W., Brűtting W. and Schwoerer M. CDW instability in the 2/1 organic conductor $(FA)_2PF_6$. *J. Phys. IV France* **1993**, 3, C2-137- C2-140.

[14] Peven P., Jérome, D., Ravy S. Albouy, P.A. and Batail P. Physical properties of the quasi-one dimensional substituted perylene cation radical salt. *Synth. Met.* **1988**, **17**, B405-B410.

[15] Ilakovac-Casses V. Etude de l'influence du désordre sur les instabilités et les propriétés physiques des conducteurs et supraconducteurs organiques. Thesis Université Paris-Sud (1994).

[16] Ilakovac V., Ravy S., Moradpour A., Firlej L. and Bernier P. Disorder and electronic properties of substituted perylene radical-cation salts, *Phys. Rev. B* **1995**, 52, 4108-4122.

[17] Reiss W., Schmid W., Gmeiner J. and Schwoerer M. Observation of charge density wave transport phenomena in the organic conductor $(FA)_2PF_6$. *Synth. Met.* **1991**, 41-43, 2261-2267.

[18] Reiss W., Brűtting W. and Schwoerer M. Charge transport in the quasi-one-dimensional organic charge density wave conductor (Fluorenthene)$_2$PF$_6$. *Synth. Met*. **1993**, 55-57, 2664-2669.

[19] Lopes E.B., Matos M.J., Henriques R.T., Almeida M. and Dumas J. Charge density wave non-linear transport in the molecular conductor (Perylene)$_2$Au(mnt)$_2$ (mnt= maleonitriledithiolate). *Europhys. Lett.* **1994**, 27, 241-246.

[20]. Ilakovac V., Ravy S., Pouget J.P., Lenoir C., Boubekeur K., Batail P., Dolanski Babic S., Biskup N., Korin-Hamzic B., Tomic S. and Bourbonnais C. Enhanced charge localization in the organic alloys [(TMTSF)$_{1-x}$ (TMTTF)$_x$]$_2$ReO$_4$. *Phys. Rev. B* **1994**, 50, 7136-7139.

[21] Gama V., Henriques R.T., Almeida M. and Pouget J.-P. Diffuse X-ray scattering evidence for Peierls and "spin-Peierls" like transitions in the organic conductors (Perylene)$_2$M(mnt)$_2$ [M= Cu, Ni, Co and Fe]. *Synth. Met.* **1993**, 55-57 1677-1682.

[22] Gama V., Henriques R.T., Almeida M., Bourbonnais C., Pouget J.-P., Jérome D., Auban-Senzier P. and Gotschy B. Structual and magnetic investigations of the Peierls transition of α-(Per)$_2$M(mnt)$_2$ with M=Fe and Co. *J. Phys. I France* **1993**, 3,1235-1244.

[23] Lopes E.B., Matos M.J., Henriques R.T., Almeida M. and Dumas J. Charge Density Wave Dynamics in Quasi-One Dimensional Molecular Conductors: a Comparative Study of (Per)$_2$M(mnt)$_2$ with M =Au, Pt. *J. Phys. I France* **1996**, 6, 2141-2149.

[24] Bonfait G., Matos M.J., Henriques R.T and Almeida M. The Peierls transition under high magnetic field. *Physica B* **1995**, 211, 297-299.

[25] Graf D., Brooks J.S.,Choi E.S.,Uji S., Dias J.C., Almeida M. and Matos M., Suppression of a charge-density-wave ground state in high magnetic fields: Spin and orbital mechanisms. *Phys. Rev. B* **2004**, 69, 125113.

[26] Brooks J.S., Graf D., Choi E.S., Almeida M., Dias J.C., Henriques R.T. and Matos M. Magnetic field dependence of CDW phases in Per$_2$M(mnt)2 (M=Au, Pt). *Journal of Low Temperature Physics* 2006, **142**, 787-803.

[27] Brooks J.S., Graf D., Choi E.S., Almeida M., Dias J.C., Henriques R.T. and Matos M. Magnetic field dependent behavior of the CDW ground state in Per$_2$M(mnt)2 (M=Au, Pt). *Current Applied Physics* **2006**, 6, 913-918.

[28] Hasegawa Y. and Fukuyama H. A theory of phase transition in quasi-one-dimensional electrons. *J. Phys. Soc. Jpn* **1986**, 55, 3978-3990.

[29] Graf D., Brooks J.S., Almeida M., Dias J.C., Uji S., Terashima and Kimata M. Evolution of superconductivity from a charge-density-wave ground state in pressurized (Per)$_2$ [Au(mnt)$_2$]. *Europhys. Lett.* **2009**, 85, 27009.

[30] Shirane G., Shapiro S.M., Comès R., Garito A.F. and Heeger A.J. Phonon dispersion and Kohn anomaly in tetratiafulvalene-tetracyanoquinodimethane (TTF-TCNQ). *Phys. Rev. B* **1976**, 14, 2325-2334.

[31] Caron L.G. and Bourbonnais C. Two-cutoff renormalization and quantum versus classical aspects for the one-dimensional electron-phonon system. *Phys. Rev. B* **1984**, 29, 4230-4241.

[32] Goze, F., Audouard A., Brossard L., Laukhin V.N., Ulmet J.P., Doublet M.L., Canadell E., Pouget J.P., Zavodnik V.E., Shibaeva R.P., Hilti B. and Mayer C.W. Magnetoresistance in pulsed fields, band structure calculations and charge density wave instability in (TSeT)$_2$Cl. *Synth. Metals* **1995**, 70, 1279-1280.

[33] Ahmad M. M., Turner D. J., Underhill A. E., Jacobsen C. S., Mortensen K. and Carneiro K. Physical properties and the Peierls instability of Li$_{0.82}$[Pt(S$_2$C$_2$(CN)$_2$)$_2$] .2H$_2$O. *Phys. Rev. B* **1984**, 29, 4796-4799.

[34] Dumoulin B., Bourbonnais C., Ravy S., Pouget J.P. and Coulon C. Fluctuation effects in low-dimensional spin-Peierls systems: theory and experiment. *Phys. Rev. Lett*. **1996**, 76, 1360-1363.

[35] Bonfait G., Matos M.J., Henriques R.T. and Almeida M. Spin-Peierls instability in $Per_2[M(mnt)_2]$ compounds probed by specific heat. *J. Physique IV Colloque* **C2-1993**, 3, 251-254.

[36] Henriques R.T., Alcacer L., Almeida M. and Tomic S. Transport and magnetic properties on the family of perylene-dithiolate conductors. *Mol. Cryst. Liq. Cryst*. **1985**, 120, 237-241.

[37] Green E. L., Brooks J. S., Kuhns P. L., Reyes A. P., Lumata L. L., Almeida M., Matos M. J., Henriques R. T., Wright J. A. and Brown S. E. Interaction of magnetic field-dependent Peierls and spin-Peierls ground states in $(Per)_2[Pt(mnt)_2]$. *Phys. Rev. B* **2011**, 84, 121101(R).

[38] Bourbonnais C., Henriques R.T., Wzietek P., Kongeter D., Voiron J. and Jerome D. Nuclear and electronic resonance approaches to magnetic and lattice fluctuations in the two-chain family of organic compounds $(perylene)_2\,[M(S_2C_2(CN)_2)_2]$ (M = Pt, Au). *Phys. Rev. B* **1991**, 44, 641–651.

[39] Green E. L., Lumata L. L., Brooks J. S., Kuhns P., Reyes A., Brown S. E. and Almeida M. $^{1}H$ and $^{195}Pt$ NMR Study of the Parallel Two-Chain Compound $Per_2[Pt(mnt)_2]$. *Crystals* **2012**, 2, 1116-1135.

[40] Pouget J.-P., Ravy S., Schoeffel J.P., Dhalenne G., and Revcolevschi A. Spin-Peierls lattice fluctuations and disorders in $CuGeO_3$ and its solid solutions.
*Eur. Phys. J. B* **2004**, 38, 581–598.

[41] Orignac E. and Chitra R. Mean-field theory of the spin-Peierls transition. *Phys. Rev. B* **2004**, 70, 214436.

[42] J.P. Pouget. Microscopic interactions in CuGeO3 and organic Spin-Peierls systems deduced from their pretransitional lattice fluctuations. *Eur. Phys. J. B* **2001**, 20, 321-333 and **2001**, 24, 415.

[43] Citro R., Orignac E. and Giamarchi T. Adiabatic-antiadiabatic crossover in a spin-Peierls chain. *Phys. Rev. B* **2005**, 72, 024434.

[44] Weiβe A., Hager G., Bishop A. R. and Fehske H. Phase diagram of the spin-Peierls chain with local coupling: Density-matrix renormalization-group calculations and unitary transformations. *Phys. Rev. B* **2006**, 74, 214426.

[45] Liu Q., Ravy S., Pouget J.P., Coulon C. and Bourbonnais C. Structural fluctuations and spin-Peierls transitions revisited. *Synth. Metals* **1993**, 55-57, 1840-1845.

[46] Eggert S., Affleck I., and Takahashi M. Susceptibility of the Spin 1/2 Heisenberg Antiferromagnetic Chain. *Phys. Rev. Lett.* **1994**, 73, 332-335.

[47] Gama V. O Papel das Cadeias Conductoras e das Cadeias Magnéticas nos Compostos da Familia $Per_x[M(mnt)_2]$ (x=2, M=Cu, Ni, Co e Fe ; x=1, M=Co). Thesis Universidade Técnica de Lisboa (1993).

[48] Alcacer L. and Maki A.H. Magnetic Properties of Some Electrically Conducting Perylene-Metal Dithiolate Complexes. *J. Phys. Chem.* **1976**, 80, 1912-1916.

[49] The spatial variation of the RKKY interaction is exactly given in 1D by: $Si(2k_Fx)-\pi/2$ , where Si is the sine integral function (see ref. [50]).

[50] Gulácsi M. "The one-dimensional Kondo lattice model at partial band filling" Advances in Physics **53** (2004) 769–937.

[51] Nomura K. and Okamoto K. Critical properties of S=1/2 antiferromagnetic XXZ chain with next-nearest-neighbour-interactions. *J. Phys. A: Math. Gen.* **1994**, 27, 5773-5788.

[52] Augier D. and Poilblanc D. Dynamical properties of low-dimensional $CuGeO_3$ and $NaV_2O_5$ spin-Peierls systems. *Eur. Phys. J. B* **1998**, 1, 19-28.

[53] Watanabe S. and Yokoyama H. Transition from Haldane Phase to Spin Liquid and Incommensurate Correlation in Spin-1/2 Heisenberg chains. *J. Phys. Soc. Japan* **1999**, 68, 2073-2097.

[54] Tsunetsugu H., Sigrist M. and Ueda K. The ground-state phase diagram of the one-dimensional Kondo lattice model. *Reviews of Modern Physics* **1997**, 69, 809-863.

[55] Xavier J.C., Pereira R.G., Miranda E. and Affleck I. Dimerization Induced by the RKKY Interaction. *Phys. Rev. Lett.* **2003**, 90, 247204.
[56] Becca F., Mila F. and Poilblanc D. Teramerization of a frustrated spin-1/2 chain. Phys. Rev. Lett. **2003**, 91, 067202.
[57] Pouget J.P. and Ravy S. Structural Aspects of the Bechgaard Salts and Related Compounds. *J. Phys. I France* **1996**, 6, 1501-1525.
[58] Pouget J.P. and Ravy S. X-Ray evidence of charge density wave modulations in the magnetic phases of $(TMTSF)_2PF_6$ and $(TMTTF)_2Br$. *Synth. Metals* **1997**, 85, 1523-1528.
[59] Foury-Leylekian P., Leininger Ph., Ilakovac V., Joly Y., Bernu S., Fagot S. and Pouget J.P. Ground state of the quasi-1D correlated electronic system $BaVS_3$. *Physica B* **2012**, 407,1692–1695
[60] Leininger Ph., V. Ilakovac, V., Joly, Y., Schierle E., Weschke E., Bunau O., Berger H., Pouget J.-P. and Foury-Leylekian P. Ground State of the Quasi-1D Compound $BaVS_3$ Resolved by Resonant Magnetic X-Ray Scattering. Phys. Rev. Lett. **2011**, 106, 167203.

Preprints (www.preprints.org) | NOT PEER-REVIEWED | Posted: 26 January 2017 doi:10.20944/preprints201701.0118.v1

Peer-reviewed version available at Magnetochemistry 2017, 3, 13; doi:10.3390/magnetochemistry3010013



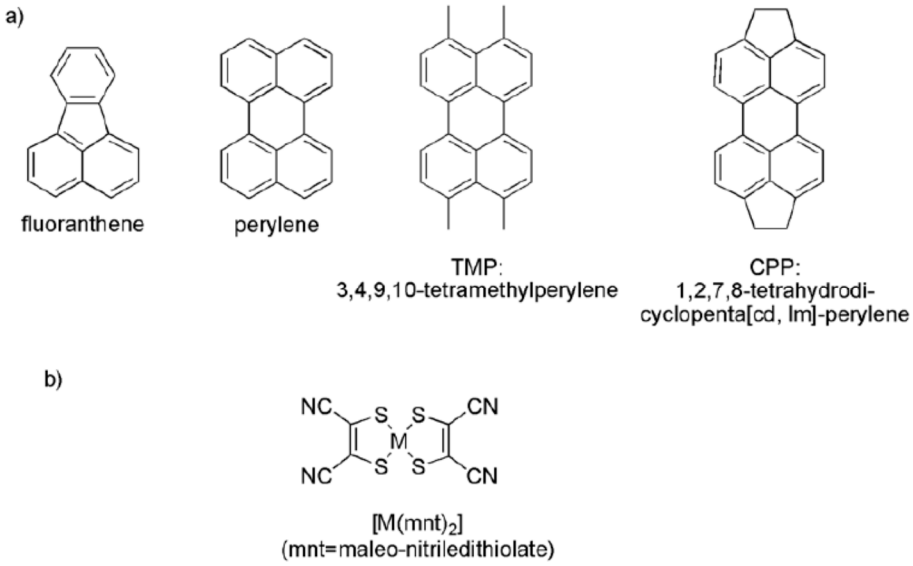


**Figure 1** Chemical structure of **(a)** fluoranthene (FA), perylene donors and its derivatives TMP and CPP and **(b)** of the dithiolate acceptor $[M(mnt)_2]$.

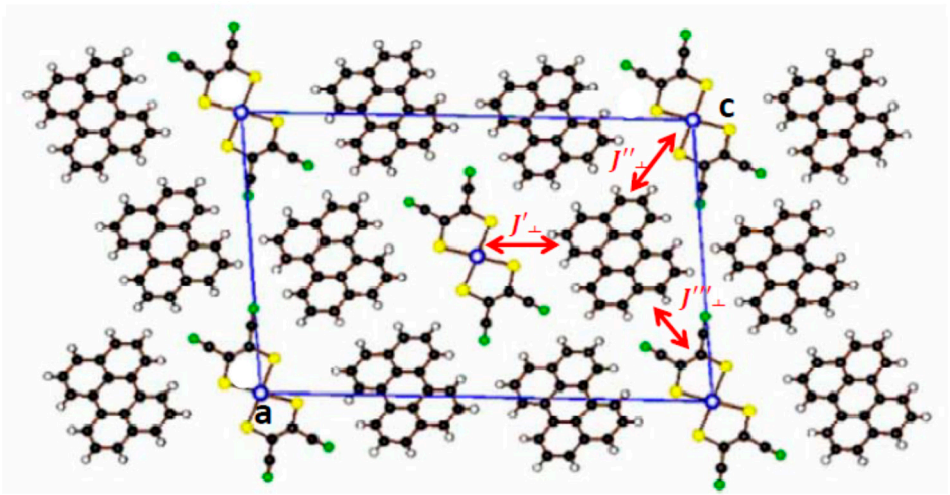


**Figure 2**

**Figure 2** Crystal structure of α- $Per_2[M(mnt)_2]$ projected along the stack direction b, and showing the formation of segregated Per and dithiolate stacks. In this structure each $[M(mnt)_2]$ stack fills tunnel delimited by 6 Per stacks, and there is one Per stack inside each triangular array of $[M(mnt)_2]$ stacks. First neighbor inter-stack $[M(mnt)_2]$ – Per AF exchange interactions $J_\perp$ are schematically indicated (note that there are three different types of interactions per Per).

Preprints (www.preprints.org) | NOT PEER-REVIEWED | Posted: 26 January 2017 doi:10.20944/preprints201701.0118.v1

Peer-reviewed version available at Magnetochemistry 2017, 3, 13; doi:10.3390/magnetochemistry3010013



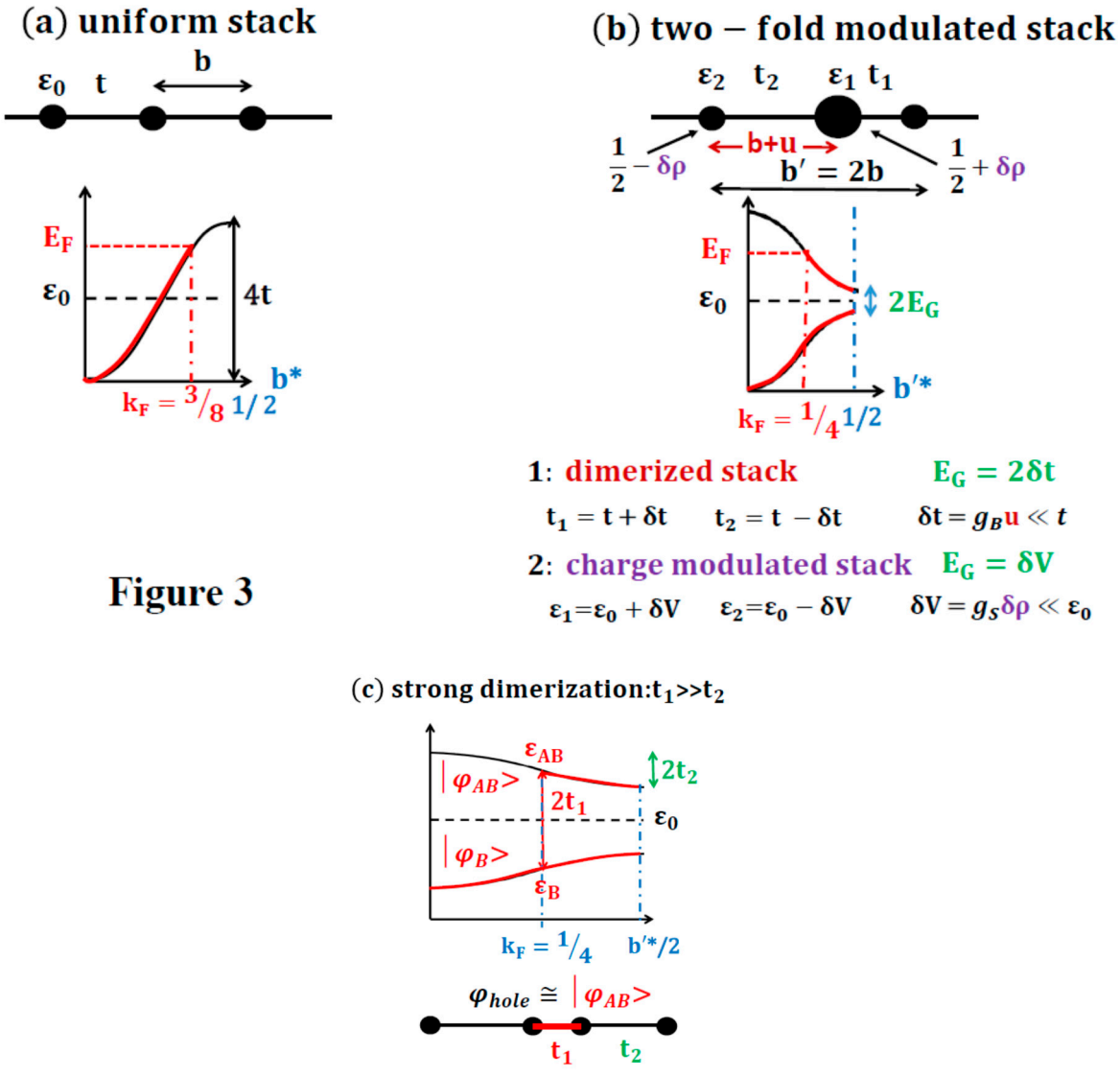


Figure 3

**Figure 3** Three-quarter electron (one-quarter hole) filled band structure of $D_2X$ arene salts for a uniform donor stack (a) and a two-fold modulated donor stack (b). The positive band dispersion is due to the graphitic type of overlap of Per molecules. In (b) the two cases of either (1) a dimerized stack or (2) a charge modulated stack are separately considered. The expression of the band gap $2E_G$ at the Brillouin zone boundary b'*/2 is given in (1) for a small modulation of transfer integrals t and in (2) for a small modulation of site energies ε. The case of a strongly dimerized stack is considered in (c). In this situation the wave functions/energies are basically that of well decoupled bonding $|\Psi_B\rangle/\varepsilon_B$ and anti-bonding $|\Psi_{AB}\rangle/\varepsilon_{AB}$ states of the dimer. For a three quarter band filling, the system can be considered has having an half-filled AB band where the hole wave function is basically localized in the anti-bonding state of the dimer.

Preprints (www.preprints.org) | NOT PEER-REVIEWED | Posted: 26 January 2017 doi:10.20944/preprints201701.0118.v1

Peer-reviewed version available at Magnetochemistry 2017, 3, 13; doi:10.3390/magnetochemistry3010013



Figure 4

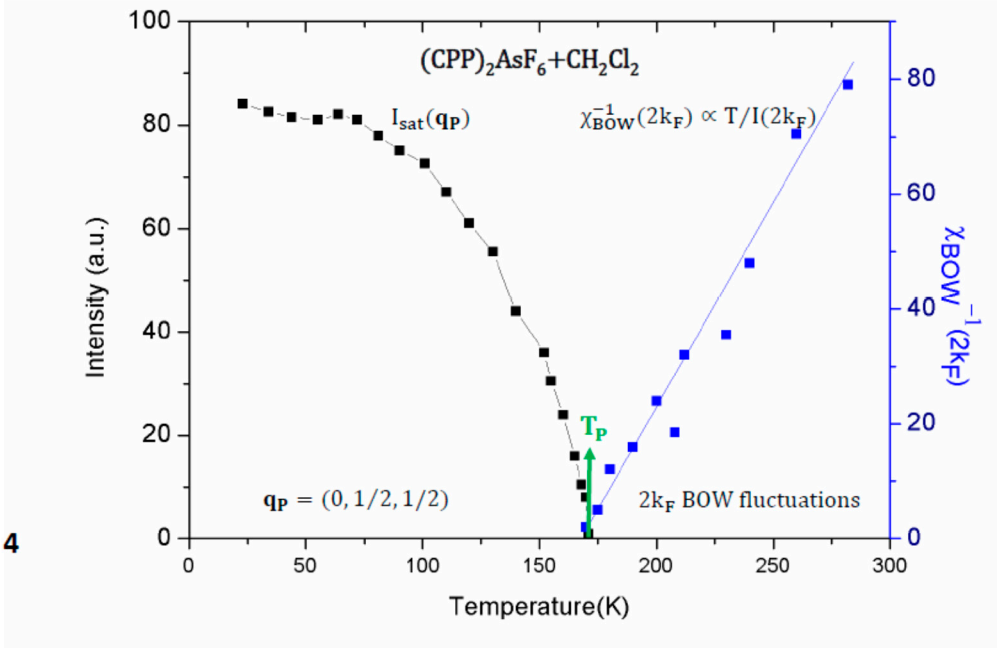


**Figure 4** Temperature (T) dependence of the inverse of the $2k_F$ BOW susceptibility $\chi_{BOW}^{-1}(2k_F)$ above $T_P$ and of the $2k_F$ Peierls satellite intensity I(**q**$_P$) below $T_P$ for $(CPP)_2AsF_6+CH_2Cl_2$ (adapted from [15, 16]). $\chi_{BOW}^{-1}(2k_F)$ is proportional to $T/I(2k_F)$, where $I(2k_F)$ is the intensity of the X-ray diffuse lines at $2k_F$.

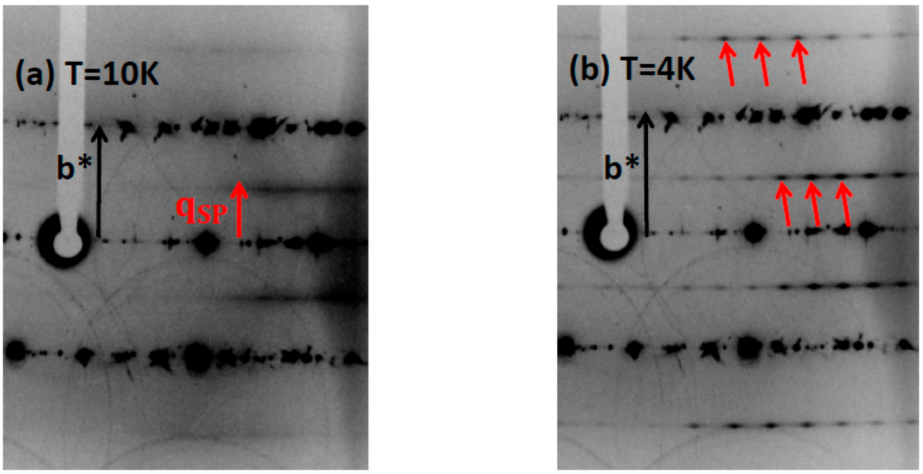


## Figure 5

**Figure 5** X-ray diffuse scattering patterns from α- $Per_2[Pt(mnt)_2]$ at 10K **(a)** and 4K **(b)**. In (a) diffuse lines due to 1D SP critical lattice fluctuations are visible between the horizontal layers of main Bragg reflections at the reduced $q_{SP}=b^*/2$ wave vector. In (b) red arrows show that these lines have condensed into broad diffuse spots, which indicates the establishment of a 3D SP SRO.

Preprints (www.preprints.org) | NOT PEER-REVIEWED | Posted: 26 January 2017 doi:10.20944/preprints201701.0118.v1

Peer-reviewed version available at Magnetochemistry 2017, 3, 13; doi:10.3390/magnetochemistry3010013



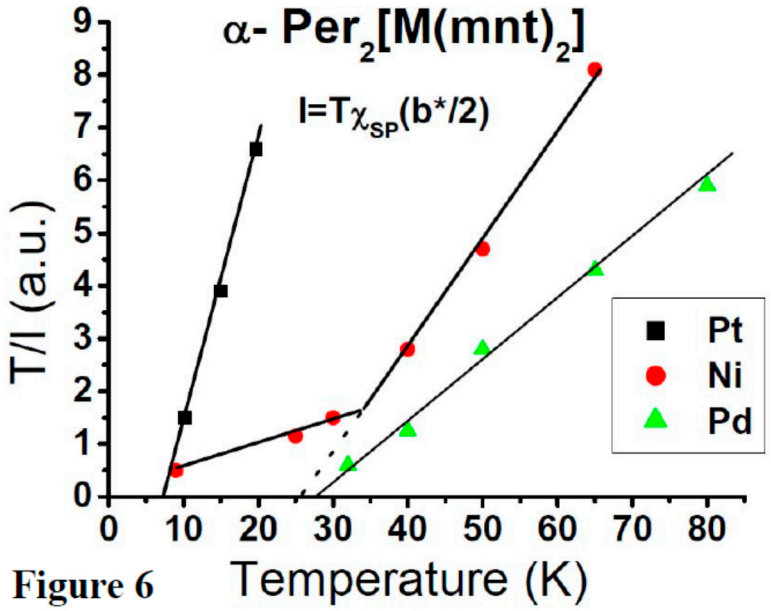


Figure 6

**Figure 6** Temperature (T) dependence of the inverse spin-Peierls susceptibility $\chi_{SP}^{-1}(q_{SP})$ for the Ni, Pd and Pt derivatives. This quantity is proportional to $T/I(q_{SP})$, where $I(q_{SP})$ is the intensity of the diffuse scattering at $q_{SP}$. $\chi_{SP}^{-1}(q_{SP})$ follows basically a Curie-Weiss law. For the Ni salt the dashed line extrapolates the thermal dependence of the high temperature data of $\chi_{SP}^{-1}(q_{SP})$ towards "$T_{SP}$".

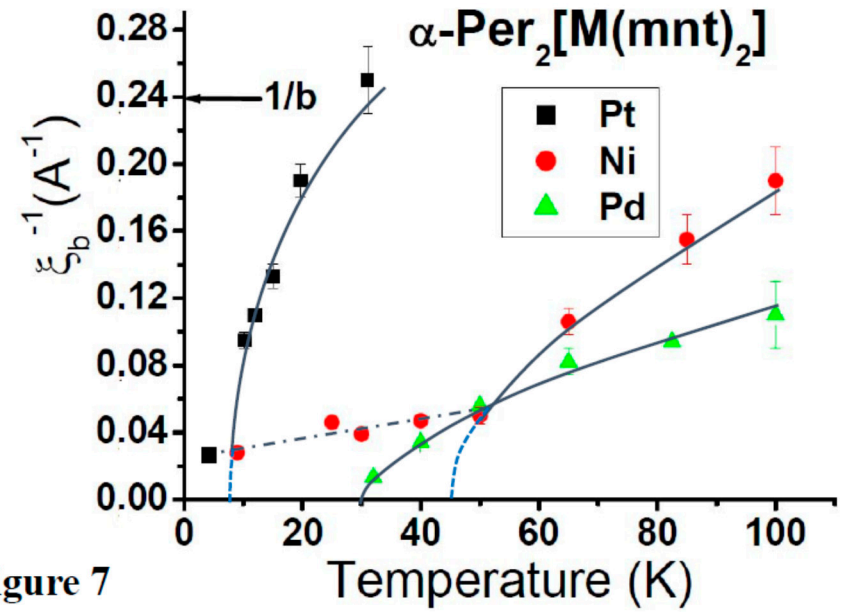


Figure 7

**Figure 7** Temperature dependence of the inverse correlation length $\xi_b^{-1}$ for the Ni, Pd and Pt derivatives. This quantity (corrected by the experimental resolution) is taken as the half width at half maximum of 1D diffuse scattering along the b direction. For the Ni and Pt salts the dashed lines extrapolate, using expression (6), the thermal dependence of the high temperature data of $\xi_b^{-1}$ towards "$T_{SP}$".

Preprints (www.preprints.org) | NOT PEER-REVIEWED | Posted: 26 January 2017 doi:10.20944/preprints201701.0118.v1

Peer-reviewed version available at Magnetochemistry 2017, 3, 13; doi:10.3390/magnetochemistry3010013



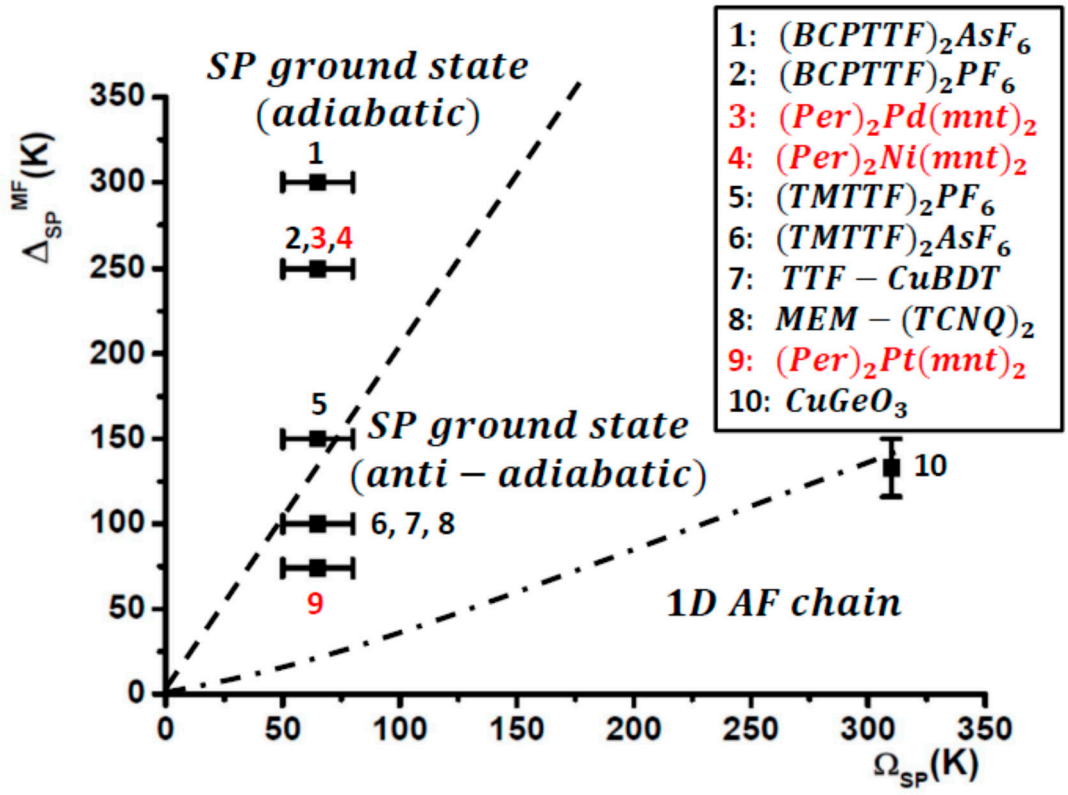


Figure 8

**Figure 8** Nature of the ground state as a function of the mean-field SP gap, $\Delta_{MF}$ defined by (7), and of the critical phonon frequency $\Omega_c$ for the SP Heisenberg chain (from [43]), together with the location of typical SP compounds (adapted from [3]). The α- $Per_2[M(mnt)_2]$ salts with M=Ni, Pd and Pt are indicated in red.

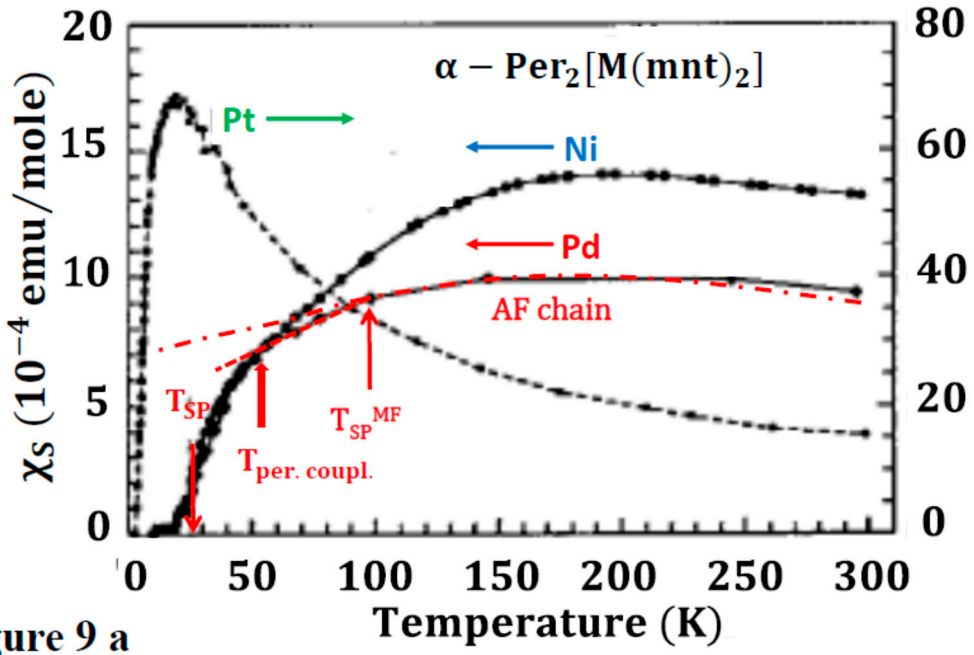


Figure 9 a

Preprints (www.preprints.org) | NOT PEER-REVIEWED | Posted: 26 January 2017 doi:10.20944/preprints201701.0118.v1

Peer-reviewed version available at Magnetochemistry 2017, 3, 13; doi:10.3390/magnetochemistry3010013



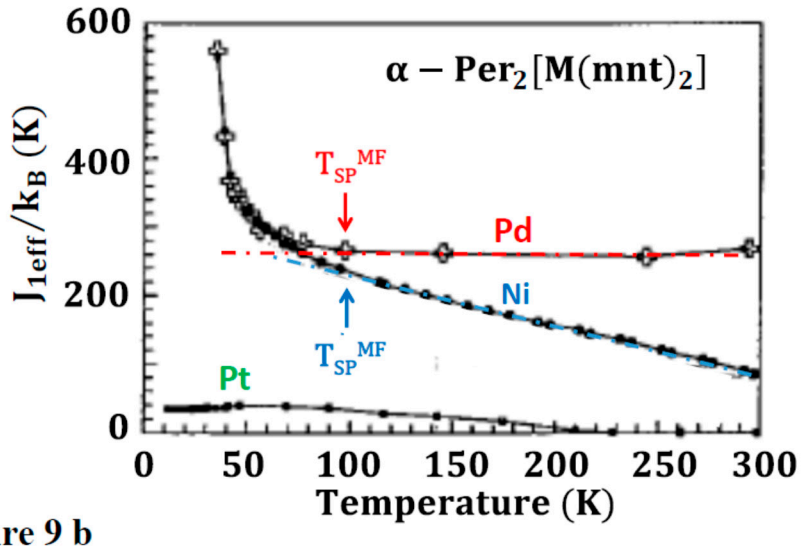


Figure 9 b

**Figure 9 (a)** Temperature dependence of the spin susceptibility, $\chi_s$ (T) of the Ni, Pd and Pt derivatives (adapted from ref. [8]). **(b)** Thermal dependence of the effective first neighbor AF exchange interaction $J_{1eff}(T)$ deduced from the amplitude of $\chi_s$ (adapted from ref. [47]). In (a), $\chi_s(T)$ of the Pd derivative can be analyzed in the following way. Above $T_{SP}^{MF} \approx 100K$ $\chi_s(T)$ follows the thermal behavior of the 1D AF chain, between $T_{SP}^{MF}$ and $T_{per.\ coupl.} \approx 50K$ the slight drop of $\chi_s(T)$ is due to the development of a pseudo-gap caused by 1D SP fluctuations on dithiolate stack, between $T_{per.\ coupl.}$ and $T_{SP} \approx 28K$ the large drop of $\chi_s(T)$ is due to an enhancement of the singlet-triplet gap due to frustration of AF interactions. A 3D SP transition occurs at $T_{SP}$. In (b), the rapid increase of $J_{1eff}(T)$ below 100K ($T_{SP}^{MF}$) occurs in the temperature range where SP fluctuations are detected.

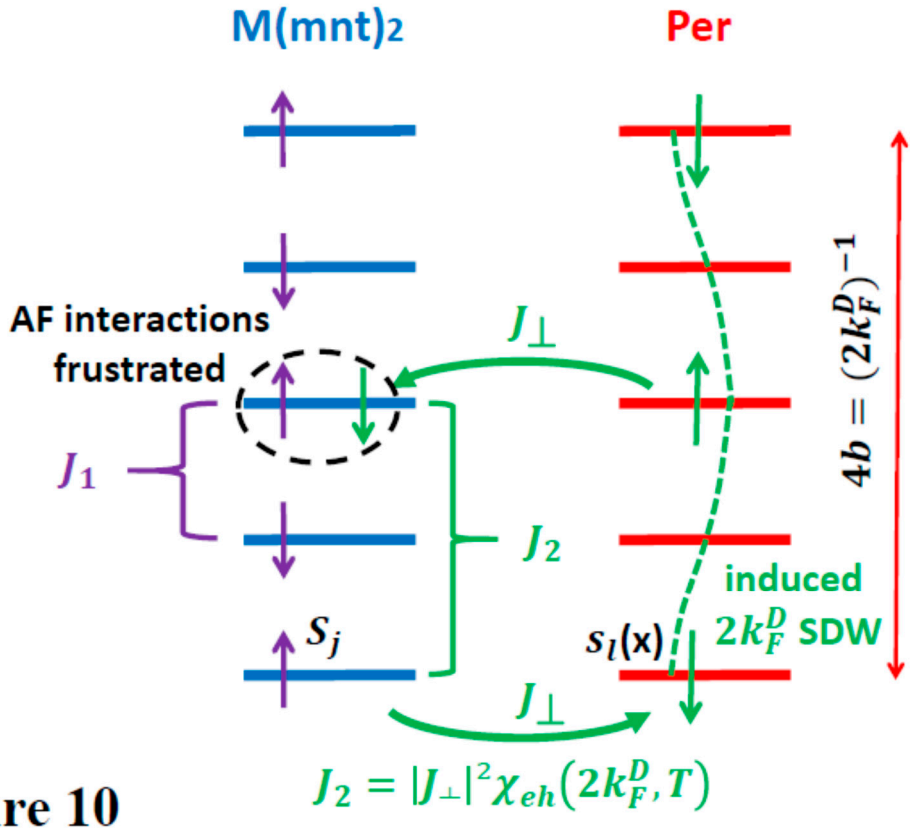


**Figure 10**

**Figure 10** Schematic representation of competing AF S=1/2 exchange couplings in α-$Per_2[M(mnt)_2]$ derivatives for M=Ni, Pd and Pt. $J_1$ is the first neighbor direct exchange coupling on dithiolate stack. $J_2$ is the second neighbor indirect RKKY exchange coupling mediated by the induced $2k_F^D$ SDW on the Per stack.